Publication No. R79-6

Order No. 632

VERTICAL AND TORSIONAL STIFFNESSES OF CYLINDRICAL FOOTINGS

by

E. KAUSEL

and

R. USHIJIMA

MIT

DEPARTMENT OF CIVIL ENGINEERING

SCHOOL OF ENGINEERING
MASSACHUSETTS INSTITUTE OF TECHNOLOGY
Cambridge, Massachusetts 02139

February 1979

Sponsored by the National Science Foundation
Division of Advanced Environmental Research and Technology
NSF-RANN Grant No. ENV 77-18339

Additional Copies May Be Obtained from
National Technical Information Service
U.S. Department of Commerce
5285 Port Royal Road
Springfield, Virginia 22121

BIBLIOGRAPHIC DATA SHEET	1. Report No. MIT-CE-79-6	2.	PB293997

4. Title and Subtitle

VERTICAL AND TORSIONAL STIFFNESSES OF CYLINDRICAL FOOTINGS

5. Report Date: February 1979

6.

7. Author(s): E. Kausel and R. Ushijima

8. Performing Organization Rept. No. R79-6; No. 632

9. Performing Organization Name and Address

Massachusetts Institute of Technology
Dept. of Civil Engineering
77 Massachusetts Avenue
Cambridge, MA 02139

10. Project/Task/Work Unit No.

11. Contract/Grant No.: NSF RANN ENV77-18339

12. Sponsoring Organization Name and Address

National Science Foundation
1800 "G" Street, N.W.
Washington, D.C. 20550

13. Type of Report & Period Covered: Research; 1978-79

14.

15. Supplementary Notes

This is the 3rd report in a series under this grant.

16. Abstracts

A numerical evaluation of the vertical and torsional stiffnesses of a cylindrical foundation embedded in an elastic stratum is presented.

Empirical formulas are given that relate stiffnesses and damping values with the embedment ratio and the depth of the stratum. Good agreement is found between the reported approximations and available analytical solutions for particular geometries.

This report constitutes a continuation of an earlier work by Elsabee and Morray in which the translation and rocking modes of vibration were studied.

17. Key Words and Document Analysis. 17a. Descriptors

soil structure interaction
dynamic stiffness of embedded foundations
consistent lateral boundaries
earthquake engineering
finite element model
soil dynamics

17b. Identifiers/Open-Ended Terms

17c. COSATI Field/Group 13 02; 8 13

18. Availability Statement	19. Security Class (This Report) UNCLASSIFIED	21. No. of Pages 93
	20. Security Class (This Page) UNCLASSIFIED	22. Price PC A04 MF A01

Massachusetts Institute of Technology
Department of Civil Engineering
Constructed Facilities Division
Cambridge, Massachusetts 02139

VERTICAL AND TORSIONAL STIFFNESSES OF CYLINDRICAL FOOTINGS

by

E. KAUSEL

and

R. USHIJIMA

February 1979

Sponsored by the National Science Foundation
Division of Advanced Environmental Research
and Technology

NSF-RANN Grant No. ENV 77-18339

Research Report R79-6 Order No. 632

ABSTRACT

A numerical evaluation of the vertical and torsional stiffnesses of an embedded cylindrical foundation is presented. The results and formulas are summarized in the section "Conclusion," in which previously reported results by Elsabee for the horizontal and rocking mode are also listed.

ACKNOWLEDGEMENT

This study was made possible by Grant ENV77-18339 of the National Science Foundation to the project entitled "Dynamic Soil-Structure Interaction."

TABLE OF CONTENTS

1. INTRODUCTION

The purpose of this work is to investigate the effects of embedment on the behavior of rigid cylindrical foundations. Simplified rules are derived to determine the static value of the vertical and torsional stiffnesses of embedded circular foundations. These rules can be utilized in preliminary analysis to assess the effects and sensitivity of the foundation to various degrees of embedment. Eventually, these formulas will be incorporated into the evaluation of the dynamic vertical and torsional stiffnesses of circular foundations.

Pioneering work in the subject of dynamically loaded, rigid, circular foundations was made by Reissner (22), Reissner and Sagoci (23) and Bycroft (6). These studies addressed the problem of surface plates underlain by elastic halfspaces or elastic strata. More recently, Luco (16) solved the problem of the torsional excitation of a rigid cylinder embedded in an elastic halfspace, and Apsel and Luco (2) gave closed-form solutions to a rigid ellipsoid of revolution embedded in a halfspace. Rigorous solutions are still lacking for the two translation modes, and for rocking of a rigid embedded cylinder.

In 1969 Tajimi (25) presented approximate equations to evaluate the motions of a rigid cylindrical body completely embedded within an elastic continuum. Approximate analytical solutions for the vertical, horizontal and rocking stiffnesses of a rigid circular footing embedded in an elastic halfspace were derived by Novak and Beredugo (20), utilizing a procedure that Novak attributes to Baranov (3). Novak (19) and Novak and Sachs (21) utilized then this procedure to obtain frequency-independent stiffnesses and damping parameters for the torsional mode. Subsequently, Bielak (5) utilized these solutions to study the behavior of structures with embedded foundations.

Contributions have been also made at various times employing finite element or finite difference solutions for strip footings and circular footings embedded in an elastic halfspace, by Kaldjian (11), Krizek, Gupta and Parmelee (14), Waas (28), Urlich and Kuhlemeyer (26), Chang-Liang (7), Kausel (12), and Johnson, Christiano and Epstein (10).

Anandakrishnan and Krishnaswamy (1), Stokoe (24) and Erden (9) as well as others have conducted experimental studies on the dynamic behavior of embedded footings.

In 1975 Elsabee (8) reported finite element solutions for circular foundations embedded in a homogeneous layer of finite depth. Approximate formulae were presented for the stiffnesses in the translational and rocking displacement modes. This study is an extension of Elsabee's work, being concerned with the determination of the static and dynamic vertical and torsional stiffnesses of an embedded circular foundation.

The solutions reported herein, as well as those by Elsabee, were obtained with a formulation and computer program developed by Kausel (12). A three-dimensional axisymmetric finite element model with transmitting boundaries was used to model a rigid, embedded circular foundation welded to a homogeneous soil deposit of finite depth resting upon a much stiffer rock-like material. The bottom boundary was, therefore, considered rigid.

The transmitting boundaries used were developed by Waas for the plane-strain case, and extended by Kausel to the three-dimensional case with axisymmetric geometry. They can be regarded as a virtual extension of the finite element mesh to infinity. This procedure has been shown to provide excellent agreement with analytical solutions even when the boundaries are placed directly at the edge of the foundation (18,28).

2. CASES STUDIED

The effects of the embedment on the static vertical and torsional stiffnesses, K_v^o and K_t^o respectively, were investigated by considering the sixteen cases listed in Table 1. The range of embedment ratios covers those values commonly encountered in the design of nuclear power plants. H is the depth of the stratum, R is the radius of the foundation, and E is the depth of the embedment (see also Fig. 1).

The value of Poisson's ratio, ν, was taken equal to 1/3 and the shear modulus, G, the radius, R, and the mass density, ρ, were equal to 1.

TABLE I

CASE	H/R	E/R	E/H
1	2	0	0
2	2	1/2	1/4
3	2	1	1/2
4	2	3/2	3/4
5	3	0	0
6	3	1/2	1/6
7	3	1	1/3
8	3	3/2	1/2
9	4	0	0
10	4	1/2	1/8
11	4	1	1/4
12	4	3/2	3/8
13	15/2	0	0
14	15/2	1/2	1/15
15	15/2	1	2/15
16	15/2	3/2	3/15

3. CORRECTION FOR MESH SIZE

When using finite elements, it is important to realize that the results obtained will be a function of the mesh size. In order to have an accurate representation of the continuum, it becomes necessary to use a sufficiently fine mesh. A more thorough approach is to utilize several mesh sizes and to extrapolate the results. Three different mesh sizes were used in this study, with square elements whose size was equal to 1/2, 1/4 and 1/6 of the foundation's radius. They will be referred to as the coarse, regular and fine meshes, respectively.

Since a linear displacement expansion procedure was used in the finite element formulation, a linear extrapolation procedure appeared to be the logical choice. Consequently, a least squares approximation was used to extrapolate the values for the vertical and torsional stiffnesses as the mesh size

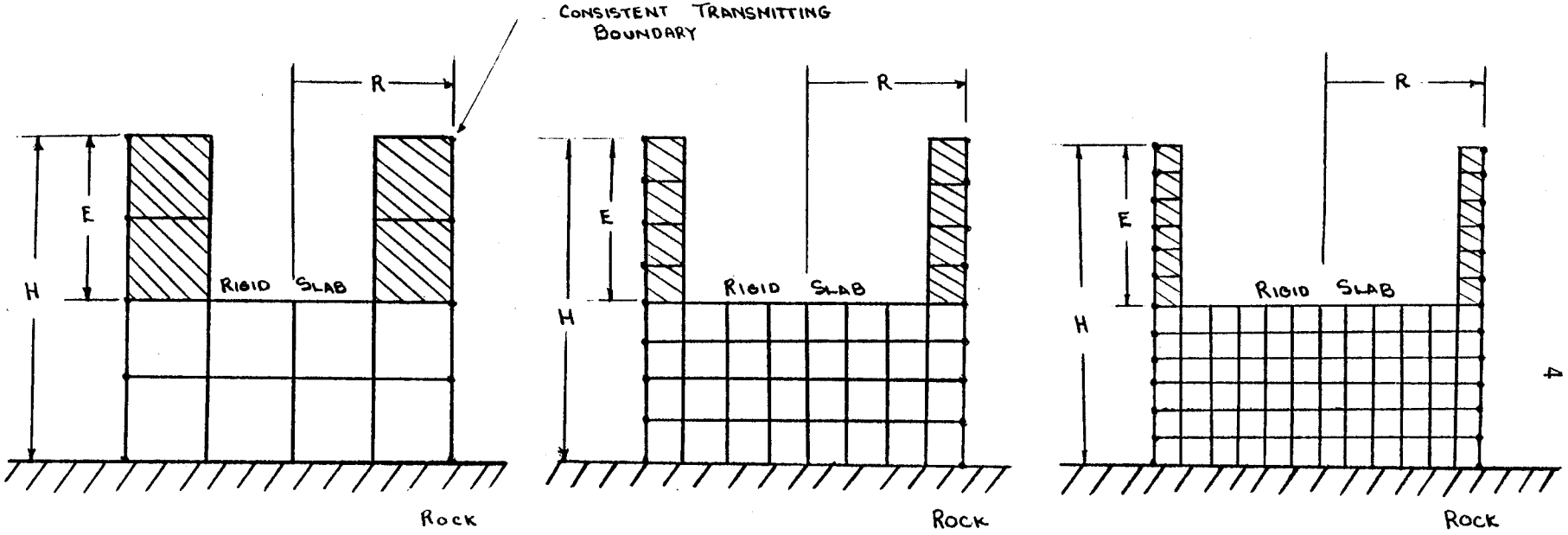

a) COARSE MESH

b) REGULAR MESH

c) FINE MESH

FIGURE 1 FINITE ELEMENT IDEALIZATION OF MASSLESS FOUNDATION

(DEPICTED WITH H/R= 2 E/R= 1)

VERTICAL STATIC STIFFNESS VERSUS MESH SIZE

FOR $H/R = 2$ $\nu = 1/3$

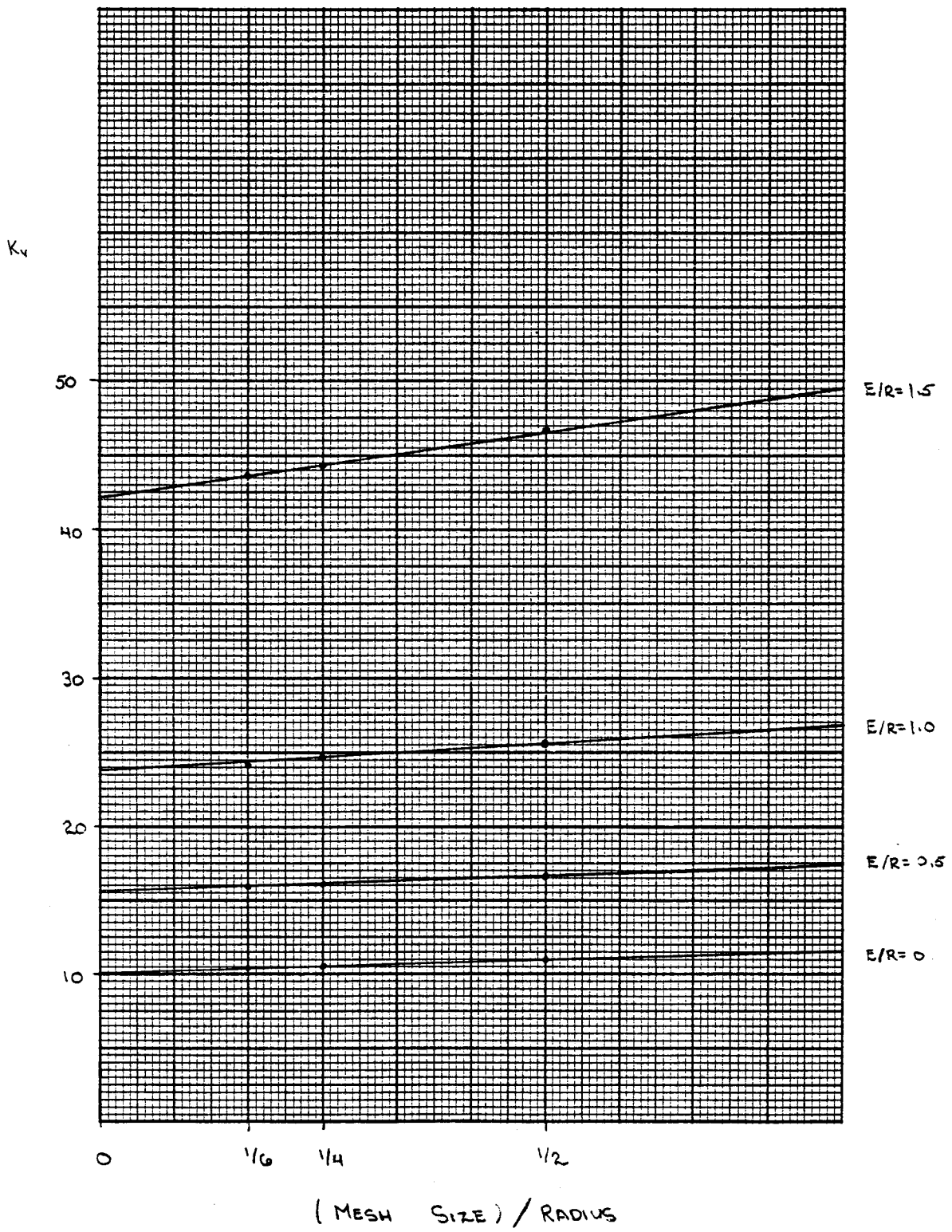

FIGURE 2

VERTICAL STATIC STIFFNESS VERSUS MESH SIZE

FOR $H/R = 3$ $\nu = 1/3$

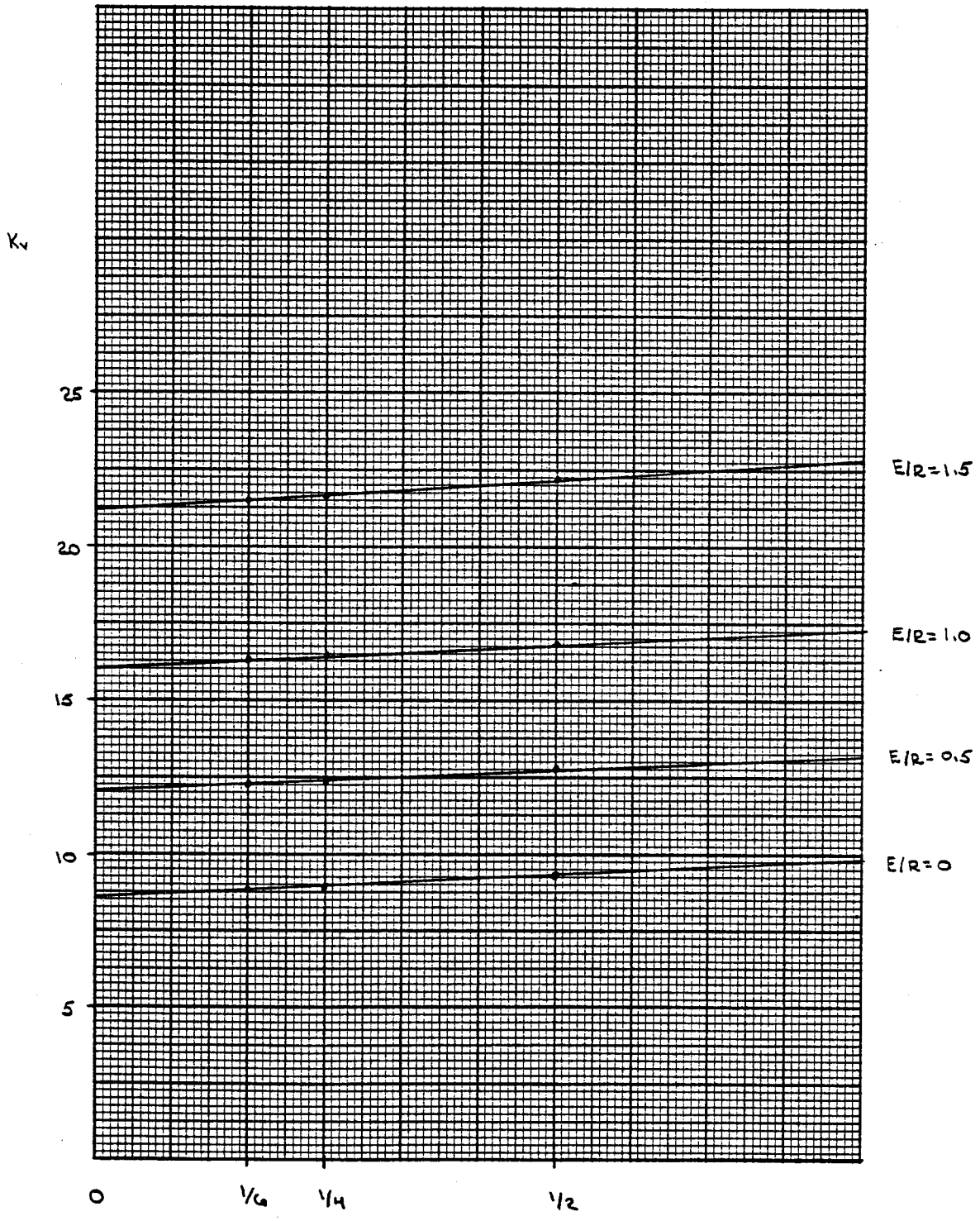

FIGURE 3

VERTICAL STATIC STIFFNESS VERSUS MESH SIZE

FOR H/R = 4 $\nu = 1/3$

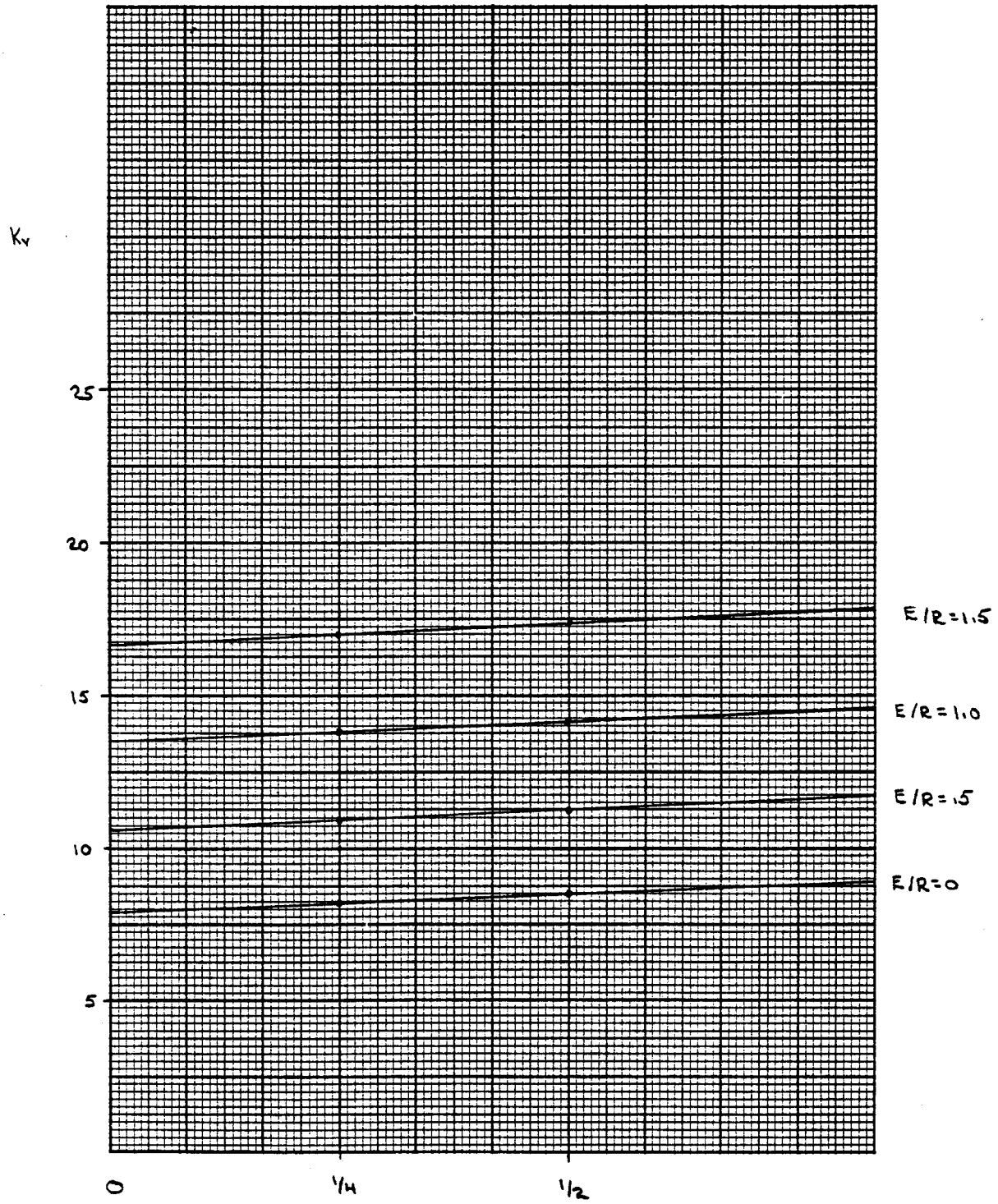

FIGURE 4

TORSIONAL STATIC STIFFNESS VERSUS MESH SIZE

FOR H/R = 2

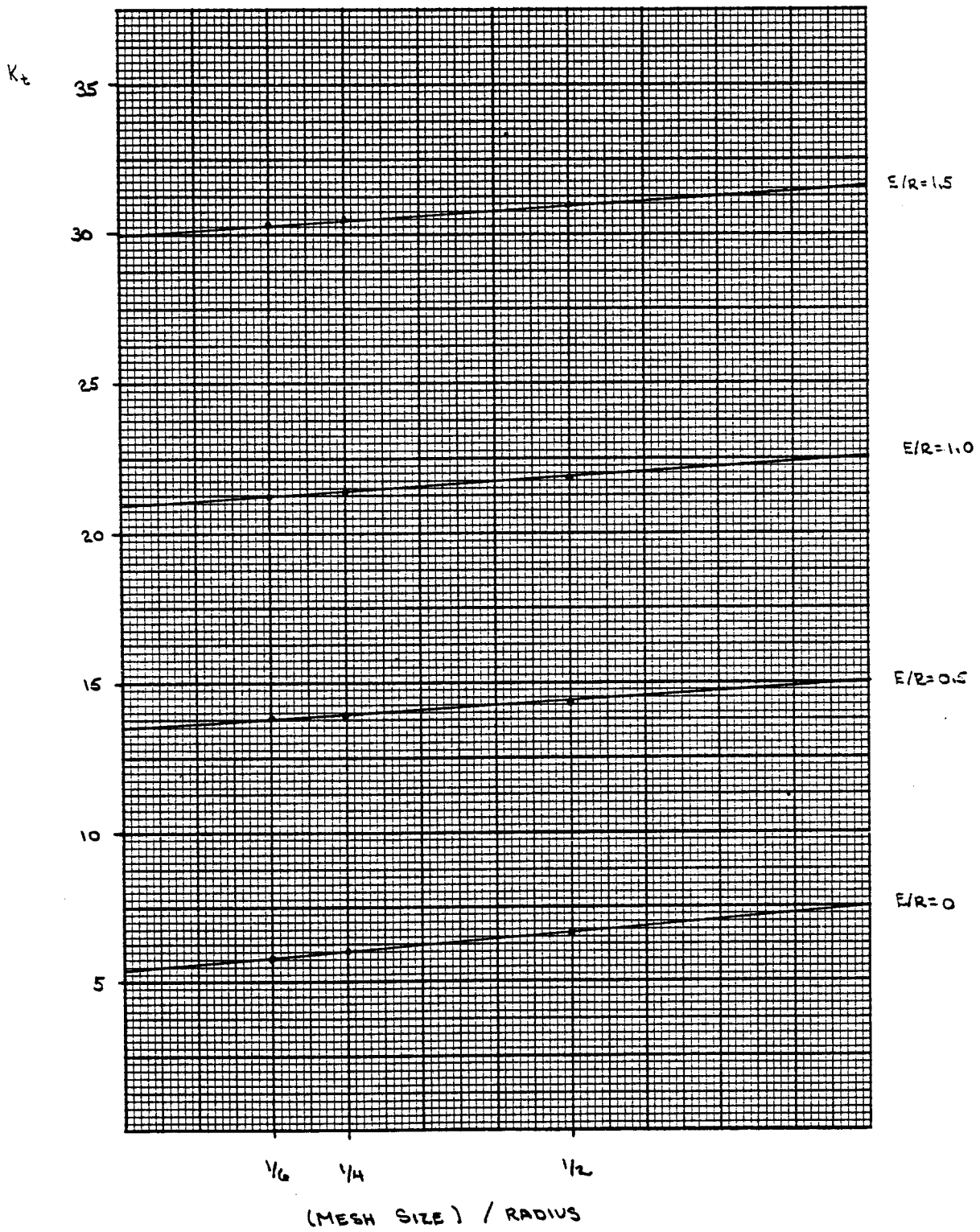

FIGURE 5

TORSIONAL STATIC STIFFNESS VERSUS MESH SIZE

FOR H/R = 3

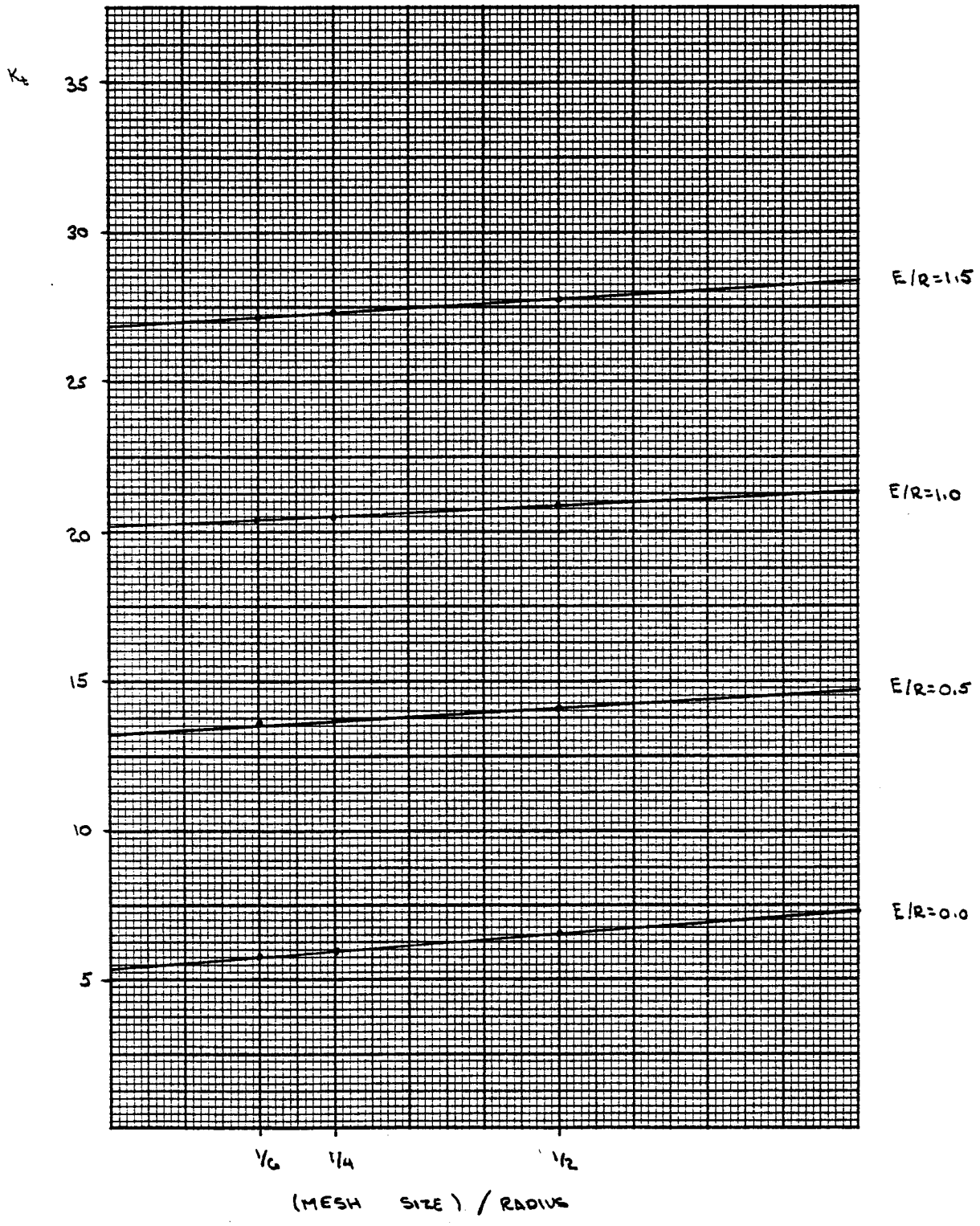

FIGURE 6

TORSIONAL STATIC STIFFNESS VERSUS MESH SIZE

FOR H/R = 4

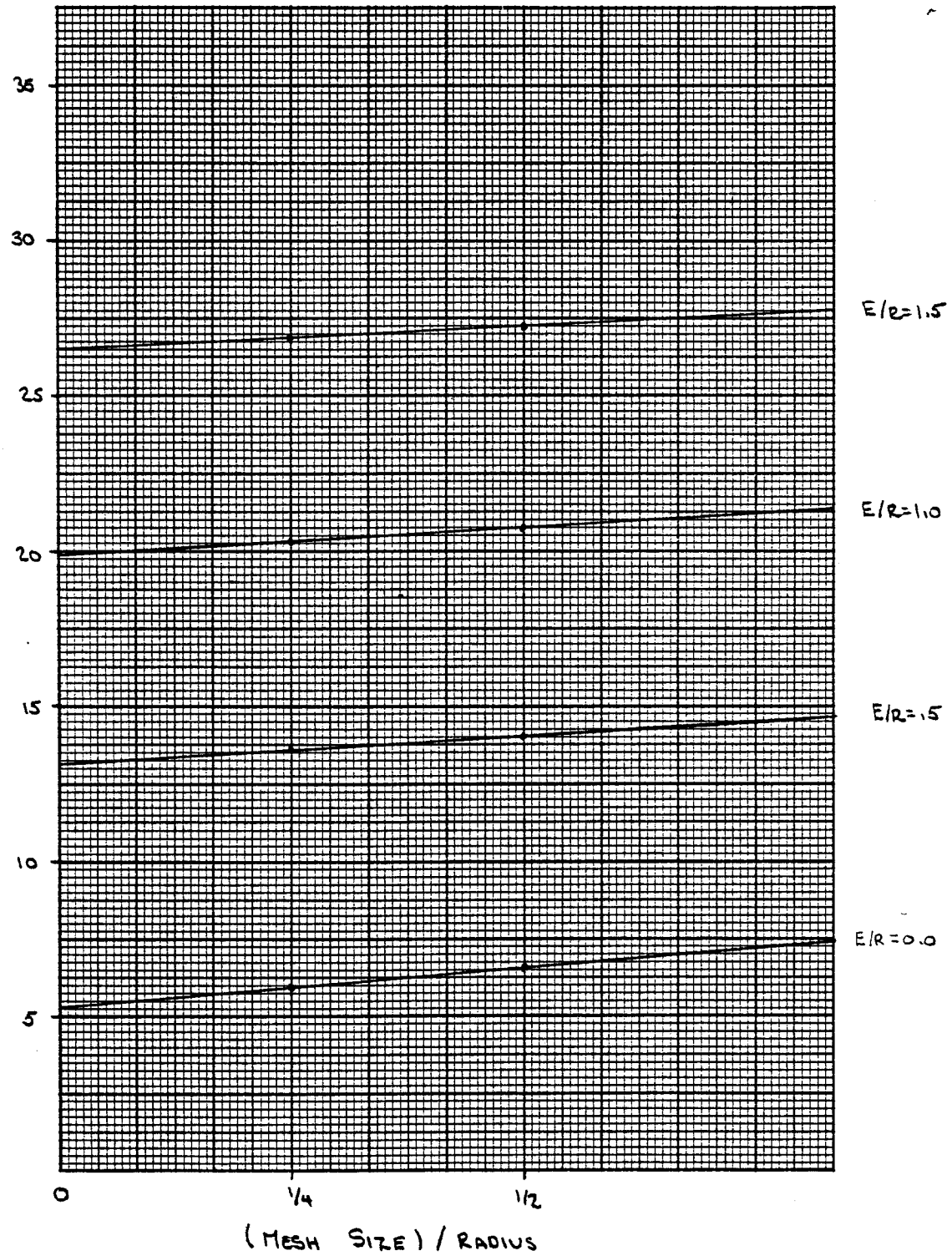

FIGURE 7

approaches zero. Figures 2 through 7 depict graphically this extrapolation procedure. Observe how closely the regression lines pass through the data points. The extrapolated data are tabulated in Tables 2 and 3, and the resulting static stiffnesses are plotted in Figures 8 and 9.

TABLE 2 - STATIC VERTICAL STIFFNESSES

		MESH SIZE			
H/R	E/R	COARSE	REGULAR	FINE	EXTRAPOLATED
2	0.0	11.08	10.58	10.41	10.08
	0.5	16.77	16.18	16.00	15.51
	1.0	25.58	24.65	24.40	23.78
	1.5	46.74	44.29	43.73	42.11
3	0.0	9.30	8.92	8.80	8.55
	0.4	12.79	12.43	12.31	12.07
	1.0	16.84	16.42	16.30	16.02
	1.5	22.23	21.49	21.54	21.18
4	0.0	8.50	8.18	—	7.86
	0.5	11.24	10.95	—	10.66
	1.0	14.09	13.79	—	13.49
	1.5	17.33	17.00	—	16.67
7.5	0.0	7.50	—	—	7.01
	0.5	9.48	—	—	9.05
	1.0	11.32	—	—	10.91
	1.5	13.15	—	—	12.82

STATIC VERTICAL STIFFNESS VERSUS R/H

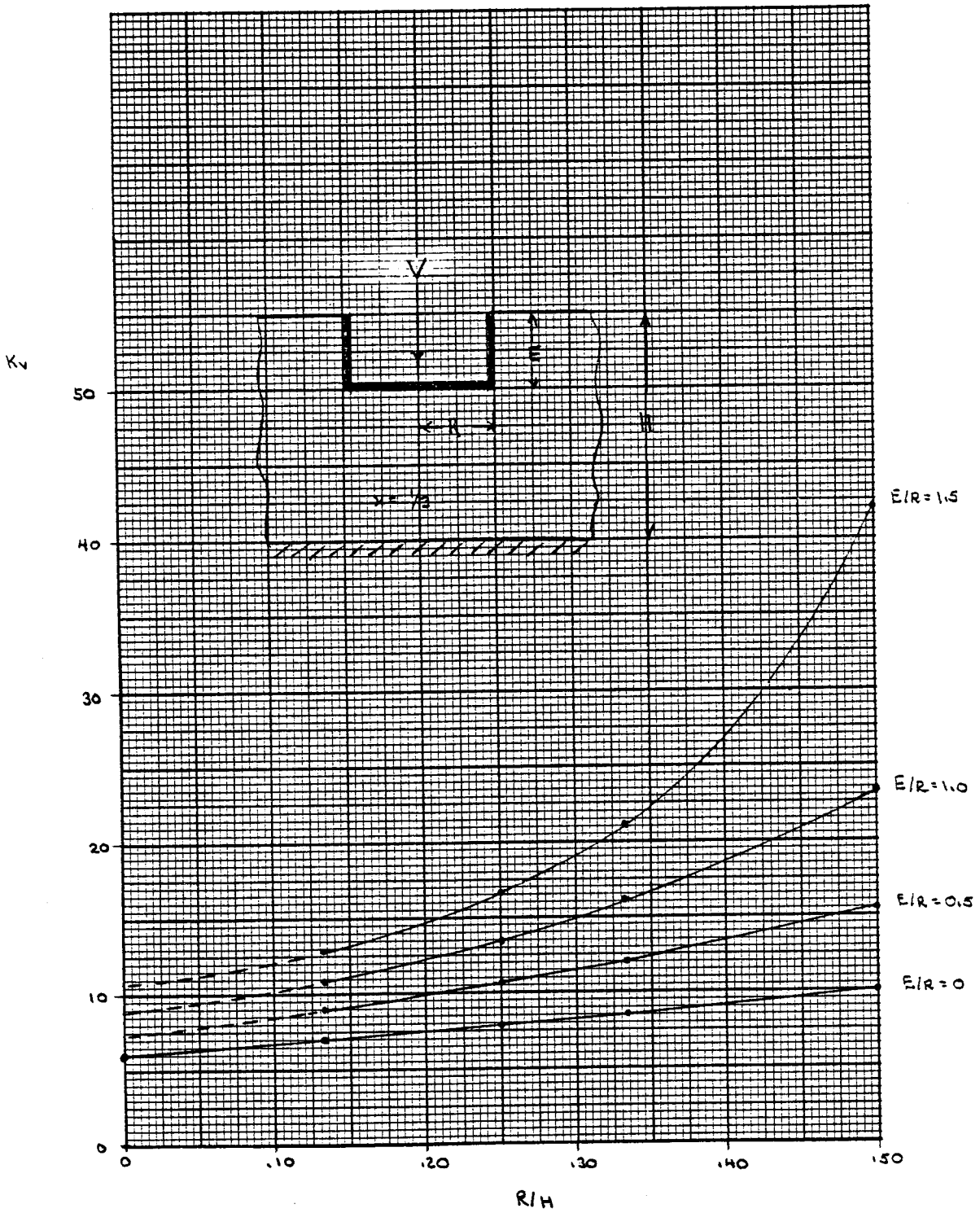

FIGURE 8

TABLE 3 - STATIC TORSIONAL STIFFNESSES

		MESH SIZE			
H/R	E/R	COARSE	REGULAR	FINE	EXTRAPOLATED
2	0.0	6.70	6.03	5.82	5.37
	0.5	14.39	13.93	13.80	13.49
	1.0	21.82	21.37	21.24	20.94
	1.5	30.97	30.45	30.30	29.95
3	0.0	6.64	5.99	5.77	5.34
	0.5	14.11	13.66	13.54	13.24
	1.0	20.93	20.50	20.38	20.09
	1.5	27.77	27.34	27.22	26.93
4	0.0	6.63	5.98	—	5.33
	0.5	14.04	13.59	—	13.14
	1.0	20.74	20.32	—	19.90
	1.5	27.33	26.92	—	26.51
7.5	0.0	6.62	—	—	5.32
	0.5	13.99	—	—	13.09
	1.0	20.63	—	—	19.78
	1.5	27.12	—	—	26.31

For values of H/R equal to 4.0, the stiffnesses of the fine mesh were not determined due to the significant computer resources that would have been required. Given the close fit of the regression line for the other cases, it is believed that this is not a source of significant error.

For values of H/R equal to 7.5, on the other hand, only the stiffnesses for the coarse mesh were evaluated. The following procedure was then utilized to obtain approximate values for the continuum: the ratios of the extrapolated stiffnesses to the stiffnesses for the coarse mesh were evaluated for the other values of H/R already obtained. Those ratios, for a particular value of E/R, were plotted as a function of R/H, and a linear

STATIC TORSIONAL STIFFNESS VERSUS R/H

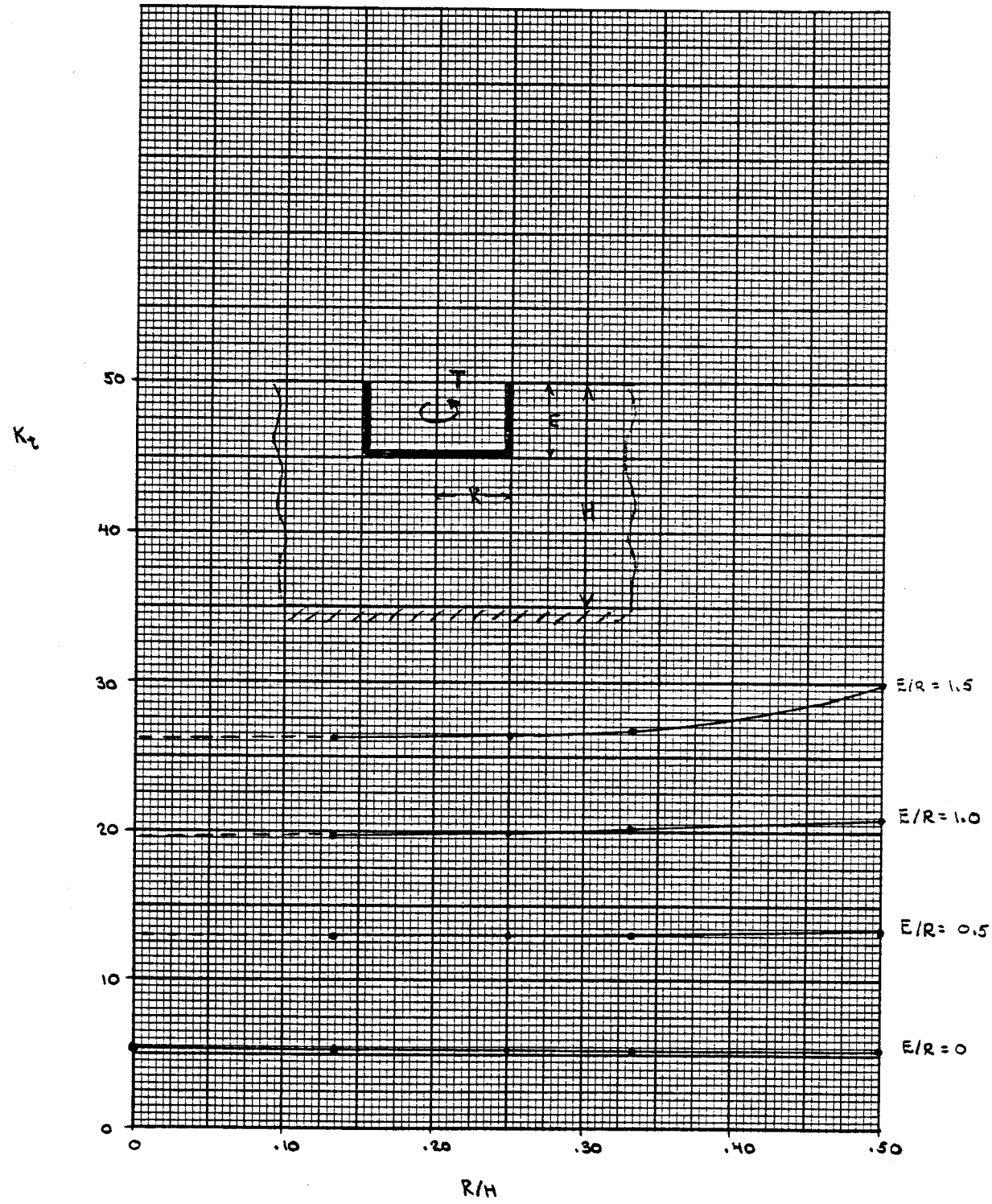

FIGURE 9

expression relating error to mesh size and the parameters E/R, R/H was determined. Thus an appropriate reduction for the coarse mesh was obtained for the various embedment ratios under consideration.

4. STATIC VERTICAL STIFFNESS

Fig. 8 shows the static vertical stiffness, as obtained by the extrapolation procedure described, versus the depth of the stratum and with the embedment ratio E/R as a parameter. Additionally, we know that the analytical solution for vertical loading of a surface plate welded to a halfspace is

$$K_v = \frac{4GR}{1-\nu} \tag{1}$$

which for $\nu = 1/3$ gives $K_v = 6GR$. This point is also shown in Fig. 8. The dashed lines correspond to the empirical expressions for the stiffnesses which are derived in the following pages.

We shall assume that the effects of embedment and strata depth are separable, so that the stiffness can be expressed as

$$K_v\left(\frac{R}{H}, \frac{E}{R}\right) = \frac{4GR}{1-\nu} \; f\left(\frac{R}{H}\right) \cdot g\left(\frac{E}{R}\right) \cdot h\left(\frac{E}{H}\right) \tag{2}$$

where f, g, h are functions to be determined, and which are such that $f(0) = g(0) = h(0) = 1$ (since $K_v(0,0) = 4GR/(1-\nu)$).

From the postulated expression, it follows that

$$f\left(\frac{R}{H}\right) = \frac{K_v\left(\frac{R}{H}, \frac{E}{R} = 0\right)}{\left(\frac{4GR}{1-\nu}\right)} \tag{3}$$

In other words, the function f gives the stiffness factor which must be applied to the theoretical halfspace value to obtain the stiffness of a rigid disk on the surface of a stratum. Fig. 10 shows the variation in stiffness for this case in terms of the depth ratio R/H. The location of the data points suggests that a straight line would be adequate to describe the increase in stiffness; the line shown in fig. 10 has the equation

STATIC VERTICAL STIFFNESS FOR ZERO EMBEDMENT (E/R = 0)

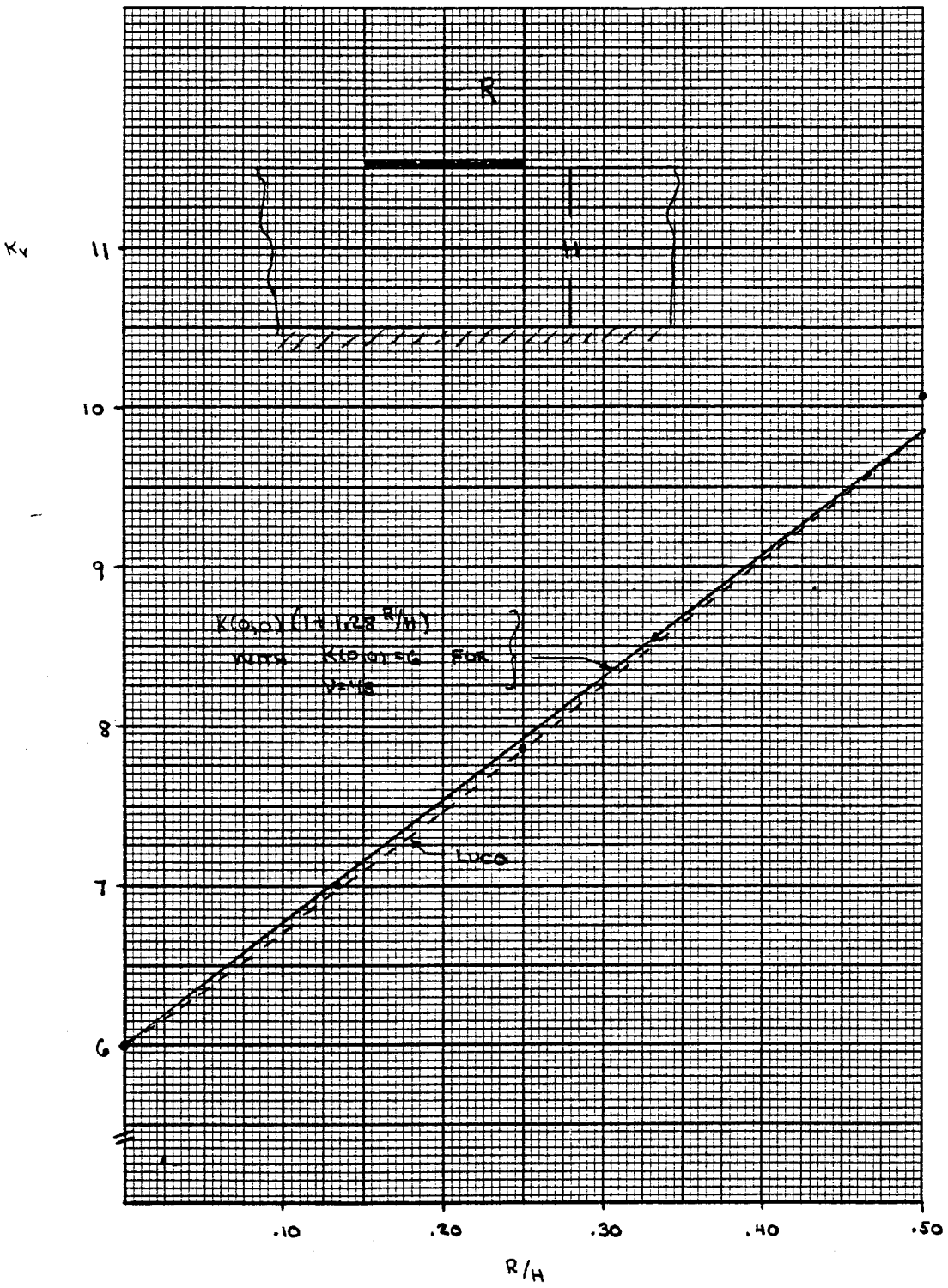

FIGURE 10

$$K\left(\frac{R}{H}, \frac{E}{R} = 0\right) = K(0,0)\left(1 + 1.28\,\frac{R}{H}\right) \qquad (4)$$

so that

$$f\left(\frac{R}{H}\right) = 1 + 1.28\,\frac{R}{H} \qquad (5)$$

To increase the confidence in this expression, a comparison was made with analytical results obtained (numerically) by Luco (15) for a rigid disk on a stratum underlain by elastic rock. To perform the comparison, it was necessary to read the static stiffnesses from fig. 10 in Luco's paper for the case having the stiffest rock, i.e., with a shear modulus equal to 29 times the shear modulus of the stratum (no results for rigid rock were presented). Luco's static stiffnesses (adapted) are shown in fig. 10 as a dashed line. The agreement with the straight line given by equation 4 is excellent.

Having determined f, we turn our attention to the second factor, namely g(E/R). It gives the relative increase in stiffness for an embedded foundation in an infinite halfspace. As of this writing, there are no closed form solutions available for the vertical stiffness of an embedded, rigid cylinder. Novak's approximate values for dynamically loaded footings (Novak, 21) were obtained assuming that the total stiffness is equal to the sum of two terms: the stiffness of a rigid disk on the surface of a halfspace and having the same radius as the cylinder, plus the stiffness of a plate of thickness E and with a hole of diameter 2R, which is subjected to forces distributed around the perimeter of the hole. This can be represented graphically as

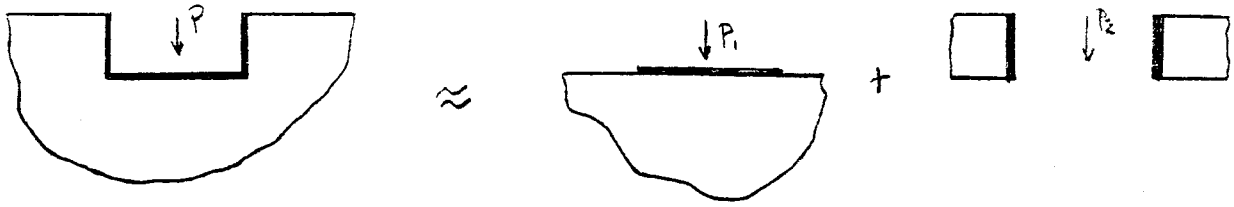

Obviously this procedure violates the boundary conditions at the interface of the plate and the halfspace. For static loads, the stiffness of the infinite plate to vertical loads is zero, leading to the surprising conclusion that embedment has no effect on the static vertical stiffness. We know, of course, that this is not the case (see fig. 8) pointing out the difficulties involved in determining the effects of embedment with simple models such as Novak's. (It is fair to add, however, that Novak's model improves for dynamic loads.)

In this work, we begin normalizing the stiffnesses by the values corresponding to E/R = 0, that is, computing the ratios

$$\frac{K(\frac{R}{H}, \frac{E}{R})}{K(\frac{R}{H}, \frac{E}{R} = 0)} \tag{6}$$

which by equation (2) should give $g(E/R) \cdot h(E/H)$. The results of this normalization are shown in fig. 11 and in table 4 in terms of R/H. The values of the functions for R/H = 0 (i.e., g(E/R)) were then determined with a quadratic extrapolation of the form $a(R/H)^2 + b(R/H) + c$, using as reference points the values of the normalized functions at R/H = 2/15, 1/4 and 1/3. It is clear that the extrapolated values are tentative, because of the uncertainties incorporated by the extrapolation procedure used. Nevertheless, when the extrapolated values are plotted as a function of E/R (fig. 12), a strong linear relationship becomes evident for moderate embedment ratios, which suggests the validity of the procedure used. On the basis of these results, it appears that an expression for g(E/R) could be chosen of the form

$$g\left(\frac{E}{R}\right) = 1 + 0.47\,\frac{E}{R} \tag{7}$$

which agrees well with the data points shown in fig. 12.

TABLE 4 - NORMALIZATION $\dfrac{K\ (R/H,\ E/R)}{K\ (R/H,0)}$

E/R	R/H				EXTRAPOLATION
	.500	.333	.250	.133	R/H = 0.0
0.0	1.000	1.000	1.000	1.000	1.000
0.5	1.549	1.418	1.356	1.292	1.234
1.0	2.359	1.874	1.716	1.559	1.471
1.5	4.178	2.477	2.121	1.829	1.790

NORMALIZED VERTICAL STIFFNESS $\frac{K(R/H, E/R)}{K(R/H, E/R=0)}$ VERSUS R/H

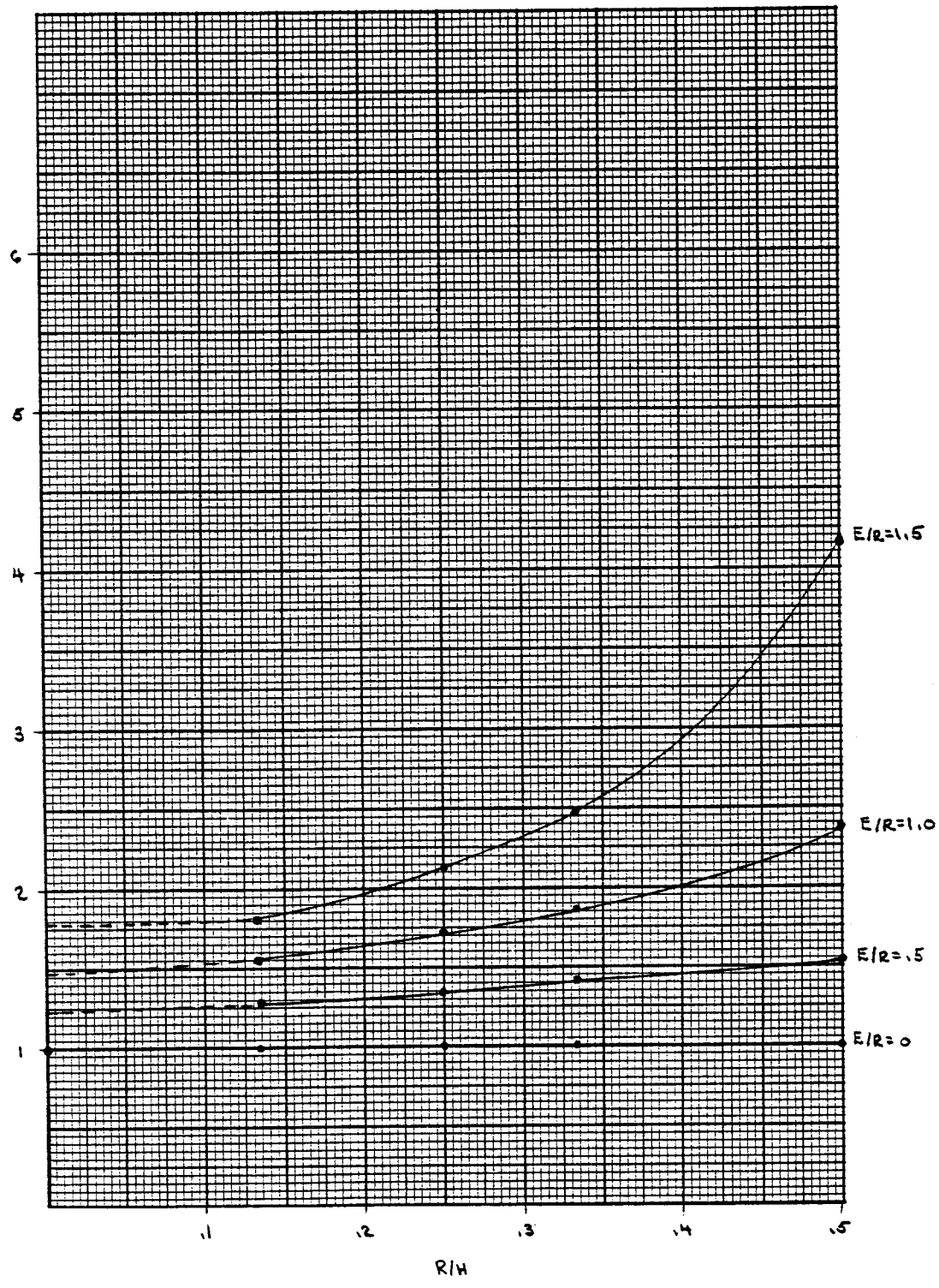

FIGURE 11

NORMALIZED VERTICAL STIFFNESS $\frac{K(R/H=0, E/R)}{K(R/H=0, E/R=0)}$ VERSUS E/R

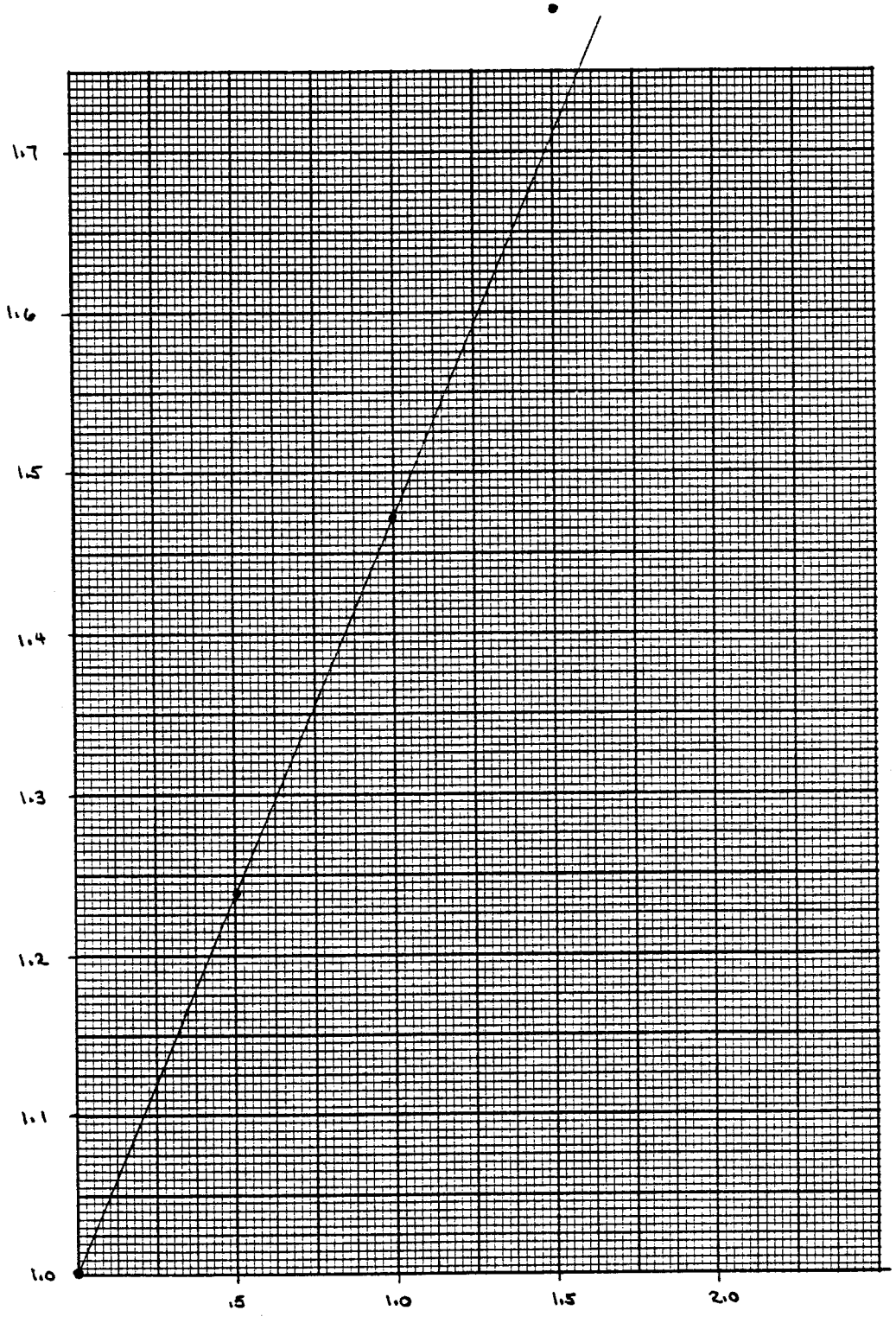

FIGURE 12

It remains only to determine expressions for h(E/H). For this purpose, we divide the data in table 4 by equation 7, determining the ratio

$$h\left(\frac{E}{H}\right) \approx \frac{K\left(\frac{R}{H}, \frac{E}{R}\right)}{K\left(\frac{R}{H}, 0\right) \cdot \left(1 + .47\,\frac{E}{R}\right)} \tag{8}$$

The results of this computation are shown in fig. 13 and in table 5. Since the stiffness approaches infinity when the depth of embedment is equal to the stratum depth, the function h(E/H) should have an asymptote at E/H = 1.

TABLE 5

E/R	H/R	E/H	$\frac{E/H}{1-E/H}$	h(E/H)
0	2	0	0	1
	3	0	0	1
	4	0	0	1
	7.5	0	0	1
.5	2	.2500	.3333	1.254
	3	.1667	.2000	1.143
	4	.1250	.1424	1.098
	7.5	.0667	.0715	1.046
1.0	2	.5000	1.0000	1.605
	3	.3333	0.5000	1.275
	4	.2500	0.3333	1.167
	7.5	.1333	0.1538	1.061
1.5	2	.7500	3.0000	2.450
	3	.5000	1.0000	1.453
	4	.3750	0.6000	1.244
	7.5	.2000	0.3600	1.073

This suggests that it might be more appropriate to plot h(E/H) in terms of E/H/(1-E/H) instead of E/H. When this is done (fig. 14), the resulting

NORMALIZED VERTICAL STIFFNESS $\frac{K(R/H,\ E/R)}{K(R/H,0)\ (1+.47\,E/R)}$ VERSUS E/H

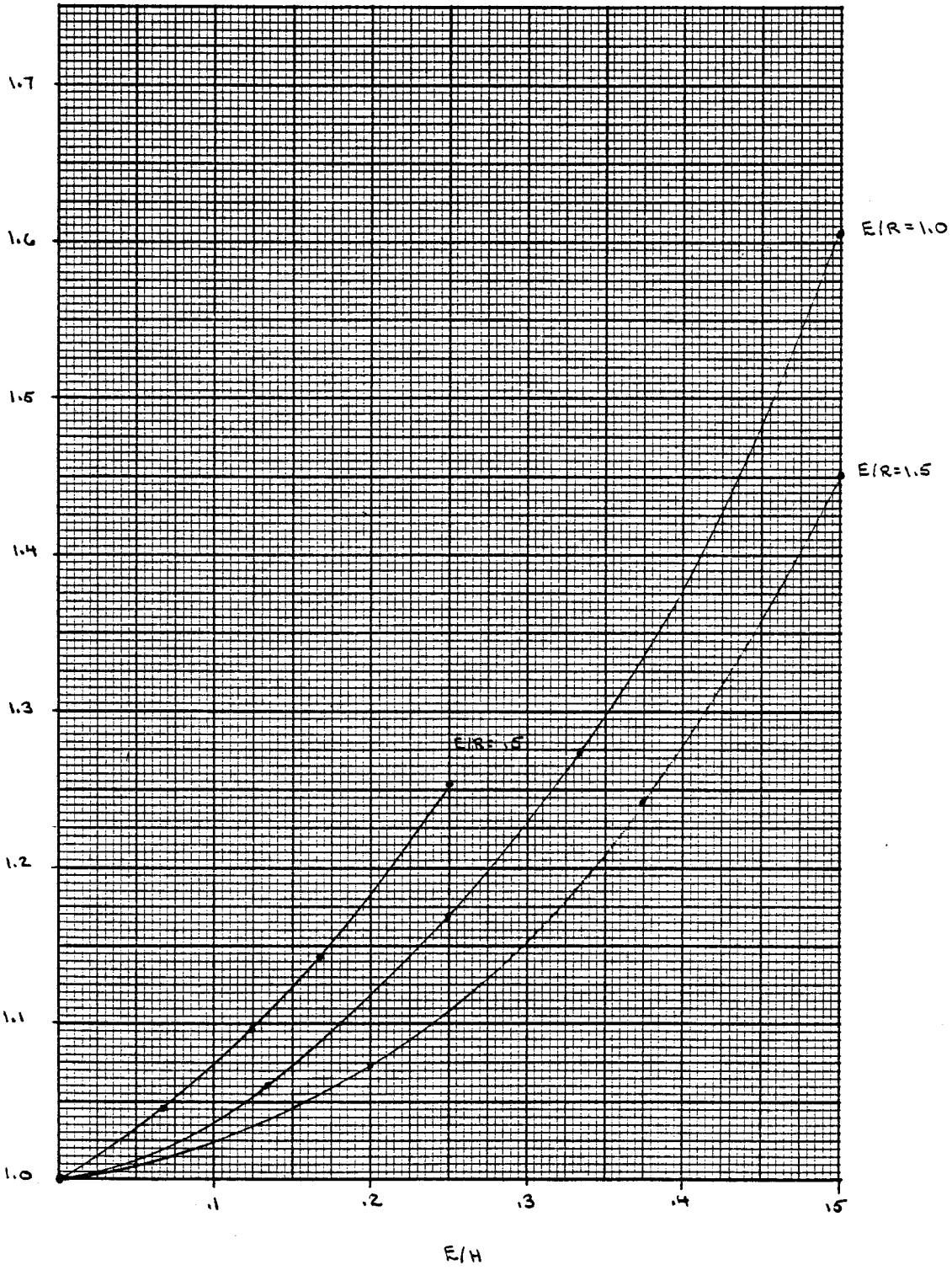

FIGURE 13

NORMALIZED VERTICAL STIFFNESS $\frac{K(R/H, E/R)}{K(R/H, 0)(1+.47\,E/R)}$ VERSUS $\frac{E/H}{1-E/H}$

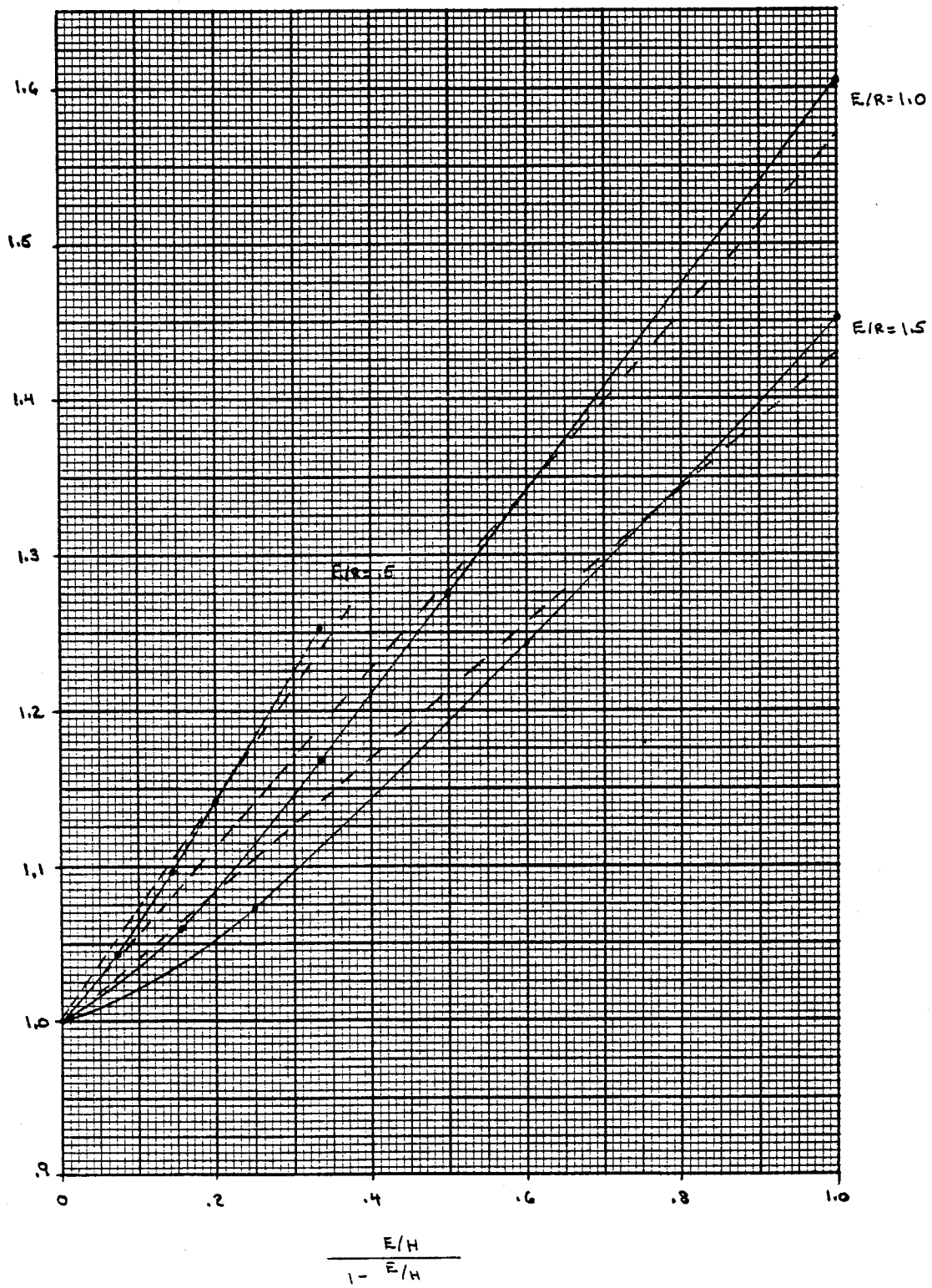

FIGURE 14

functions have less curvature, being nearly linear for large values of the abscissa. An evaluation of these curves led then to an approximation for h(E/H) of the form

$$h(E/H) = 1 + \frac{0.85\ (1 - 033\ E/R)(E/H)}{(1 - E/H)} \qquad (9)$$

which corresponds to the dashed lines in fig. 14. The fit of the approximation is not as good as for the other functions (f,g), but the relative error is still small, and certainly acceptable for practical purposes. Other expressions for h(E/H) were tried which gave a significantly better fit, but they were dismissed because they were too complicated and not warranted by the limited information available.

Combination of equations (5), (7) and (9) gives then the following empirical expression for the static vertical stiffness of a rigid, embedded cylinder:

$$K_v = \frac{4GR}{1-\nu}\ (1 + 1.23\ R/H)\ (1 + 0.47\ E/R)\ \left(1 + (0.85 - 0.28\ E/R)\ \frac{E/H}{1-E/H}\right)$$

$$(E/R < 1.5, \qquad E/H < 0.75) \qquad (10)$$

Figure 15 compares the values of K_v computed with the formula above with the original data obtained by the finite element procedure. The solid lines are identical to those in Fig. 8, while the dashed lines correspond to equation (10). Table 6, on the other hand, gives the comparison in numerical form, and lists the relative error as well. It can be seen that equation 10, while relatively simple in structure, reproduces the data points extremely well. The typical error is less than 5%, while the largest error is of the order of 10%. These values are certainly acceptable for engineering purposes, particularly when consideration is given to other uncertainties such as layering, soil properties and detachment of the lateral walls.

Admittedly, equation (10) was derived for a single value of Poisson's ratio ($\nu = 1/3$), and the functions f,g,h may depend on this ratio as well. However, on the basis of Elsabee's results for horizontal translation of an embedded cylinder, in which more values of Poisson's ratio were considered, it is felt that the effect of this parameter on f,g,h is likely to be small.

STATIC VERTICAL STIFFNESS

COMPARISON BETWEEN THE "EXACT" FINITE ELEMENT VALUES AND EQUATION 10

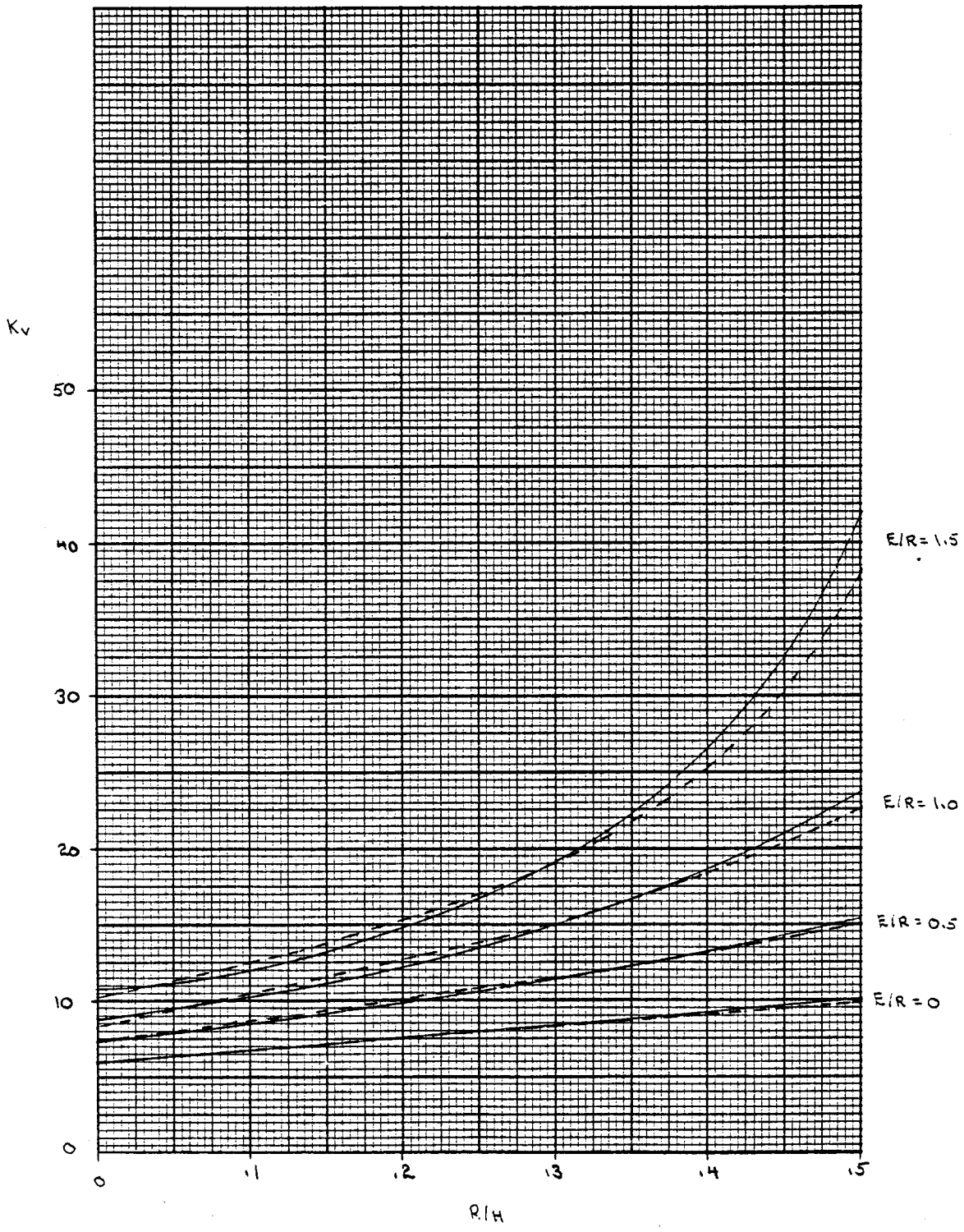

FIGURE 15

TABLE 6

E/R	H/R	"EXACT"	Equation 10	Error %
0	2	10.08	9.84	-2.4
	3	8.55	8.56	.1
	4	7.86	7.92	.8
	7.5	7.01	7.02	.2
5	2	15.61	15.02	-3.8
	3	12.07	12.07	0.0
	4	10.66	10.77	1.0
	7.5	9.05	9.11	.7
1.0	2	23.78	22.66	-4.7
	3	16.02	16.14	.8
	4	13.49	13.84	2.6
	7.5	10.92	11.23	2.8
1.5	2	42.11	37.29	-10.1
	3	21.18	20.64	-2.6
	4	16.67	18.17	9.0
	7.5	12.82	13.15	2.5

5. STATIC TORSIONAL STIFFNESS

While a closed form (numerically evaluated) solution to the problem of torsion of a rigid cylinder embedded in an elastic halfspace has been reported by Luco (16), it is of interest to apply the procedure described in earlier sections to this same problem for at least two reasons. First, solutions to the corresponding problem of a rigid cylinder in an elastic stratum are still lacking, and second, it provides an opportunity to test the procedure against accurate data, thus enhancing the confidence in the results obtained earlier, as well as in those by Elsabee.

The torsional problem is, in some sense, better behaved than the vertical problem. For one thing, it is independent of Poisson's ratio. Also

the Novak-Sachs model referenced earlier (separating the problem into a rigid disk and a free plate) works extremely well, with errors of less than 12% when compared to Luco's results. This implies that an empirical expression of the form

$$K_t = \frac{16GR}{3} f(\frac{R}{H})\ g(\frac{E}{R})\ h(\frac{E}{H}) \qquad (11)$$

with a linear function, g, should give good results to approximate the curves in fig. 9. The coefficient in front of f corresponds to the torsional stiffness of a disk on an elastic halfspace, as determined by Reissner and Sagoci (23). It is shown as an additional point in Fig. 9 for R/H = 0, E/R = 0.

Inspection of Fig. 9 reveals that embedment has a significant effect on the torsional stiffness (assuming no separation of the lateral walls to the surrounding fill!). The depth of the stratum, on the other hand, appears to have only minor influence, even for very shallow soils and deep embedment. In particular, for the case of zero embedment, the depth of the stratum (within the range of values studied) has no measurable influence; the line for E/R = 0.0 in fig. 9 is horizontal. Thus

$$f(\frac{R}{H}) = 1 \qquad \text{for any } \frac{R}{H}\ . \qquad (12)$$

Determination of an approximate expression for g(E/R) and h(E/H) was conducted in a manner similar to that applied for the vertical stiffness, dividing the actual stiffnesses by the stiffnesses corresponding to zero embedment, extrapolating the results to the case R/H = 0, and fitting empirical expressions to the normalized data. The results are presented in table 7 and fig. 16.

Table 7 - $\frac{K(R/H,\ E/R)}{K(R/H,\ 0)}$

E/R	R/H				Extrapolation	Luco (16)
	.500	.333	.250	.133	R/H=0	R/H=0
0.0	1.000	1.000	1.000	1.000	1.000	1.000
0.5	2.512	2.479	2.465	2.461	2.459	2.48
1.0	3.899	3.752	3.734	3.718	3.712	3.73
1.5	5.577	5.043	4.974	4.945	4.934	4.94

NORMALIZED TORSIONAL STIFFNESS $\frac{K(R/H, E/R)}{K(R/H, 0)}$ VERSUS R/H

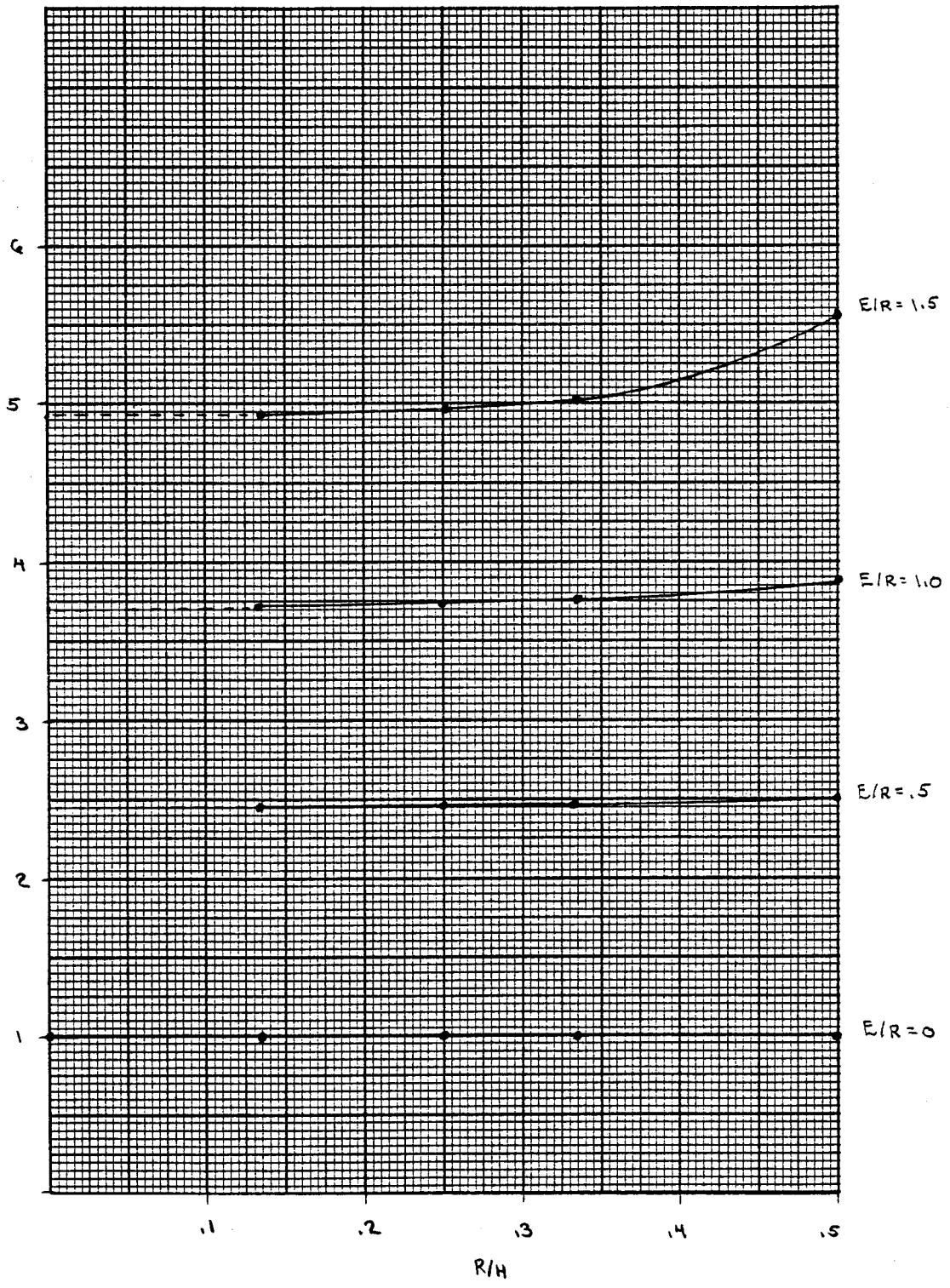

FIGURE 16

NORMALIZED TORSIONAL STIFFNESS $\frac{K_{(R/H=0,\ E/R)}}{K_{(R/H=0,\ E/R=0)}}$ VERSUS E/R

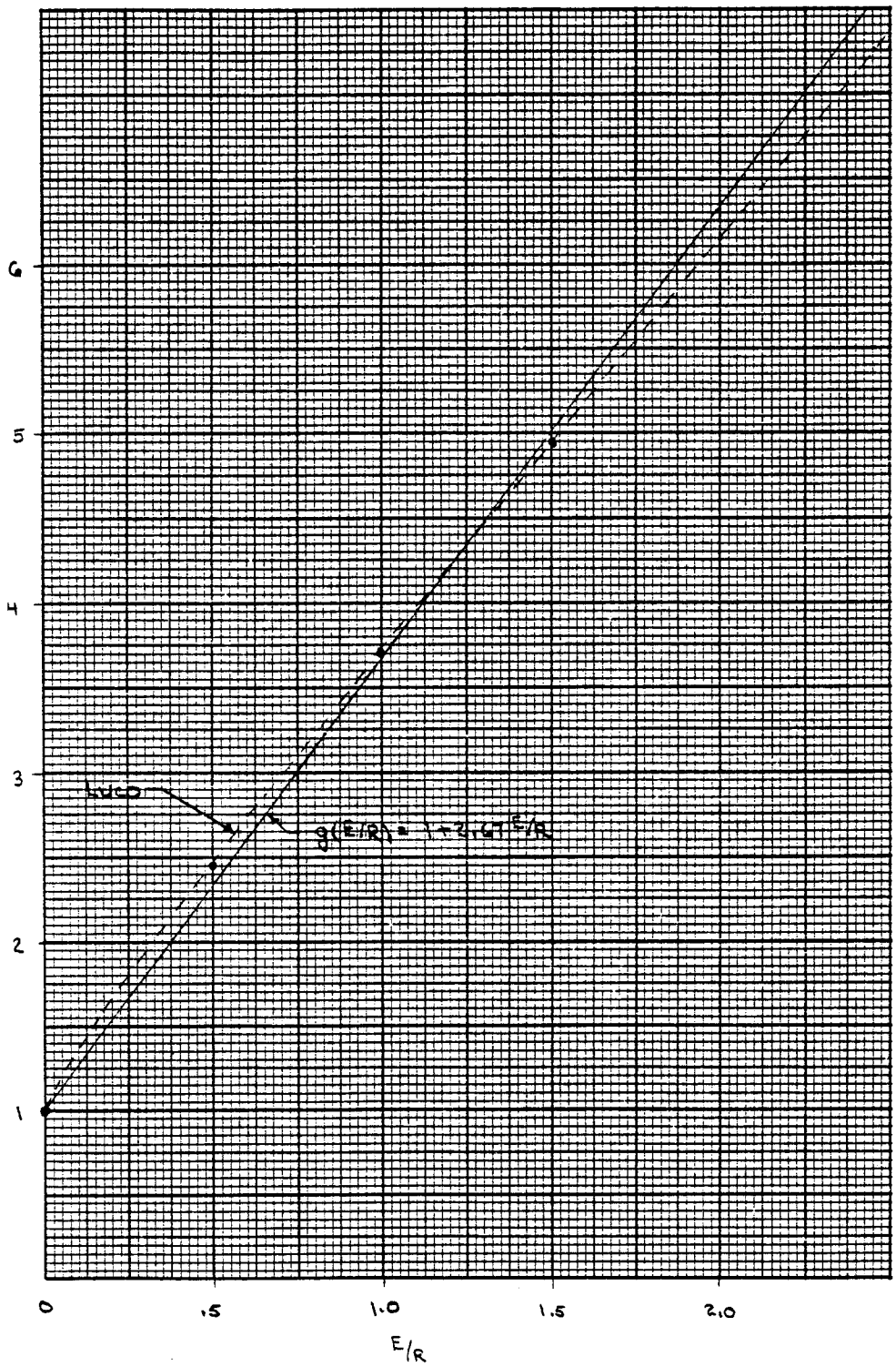

FIGURE 17

The values of the function in table 7 for R/H = 0 (i.e., g(E/R)) were obtained with a quadratic extrapolation of the form $a(R/H)^2 + c$ using as pivots the values at R/H = .133 and R/H = 0.250. The extrapolated values are plotted as dots in Fig. 17. It is apparent that, within the range of values studied, we can choose a linear approximation for g(E/R) of the form

$$g(E/R) = 1 + 2.67(E/R) \tag{13}$$

This relationship is also plotted in Fig. 17 as a solid line. The maximum error introduced by adopting this approximation is of the order of 5%. As noted earlier, Luco presented closed form solutions for the torsional stiffness of a rigid cylinder embedded within an elastic half-space. Partial results of his work, applicable to this study, are also tabulated in Table 7 and displayed as a dashed line in Fig. 17.

Agreement between Luco's analytical results and the finite element study is extremely good. The close correlation lends confidence not only to the extrapolation procedure just employed, but to the empirical expressions for the vertical stiffnesses obtained earlier.

It remains only to determine expressions for h(E/H). This may be done by computation of the ratio

$$h\left(\frac{E}{H}\right) = \frac{K(R/H,\ E/R)}{K\left(\frac{R}{H},\ E/R = 0\right)} \div \frac{K(R/H = 0,\ E/R)}{K\left(\frac{R}{H} = 0,\ E/R = 0\right)} \tag{14}$$

which follows from table 7 dividing the column data for $R/H \neq 0$ by the values corresponding to the column R/H = 0. This normalization is summarized in Table 8, and displayed in Figs. 18 and 19 in terms of E/H, and E/H/(1 - E/H) respectively. These figures demonstrate that the function h(E/H) may not be approximated by simple empirical expressions, and certainly not by linear expressions. Fortunately, the effect of this factor is very small, with typical values close to unity (see Table 8), even for the case of deep embedment in a shallow stratum. Thus, it is better to ignore the effects of this factor than to fit complicated (and unwarranted) expressions through the point data. The error incurred thereby is generally less than 10%. In view of the above, we obtain the following empirical expressions for the static torsional stiffness of a rigid, embedded cylinder:

NORMALIZED TORSIONAL STIFFNESS $h(E/H) = \frac{K(R/H, E/R)}{K(R/H, E/R=0)} \div \frac{K(R/H=0, E/R)}{K(R/H=0, E/R=0)}$

VERSUS E/H

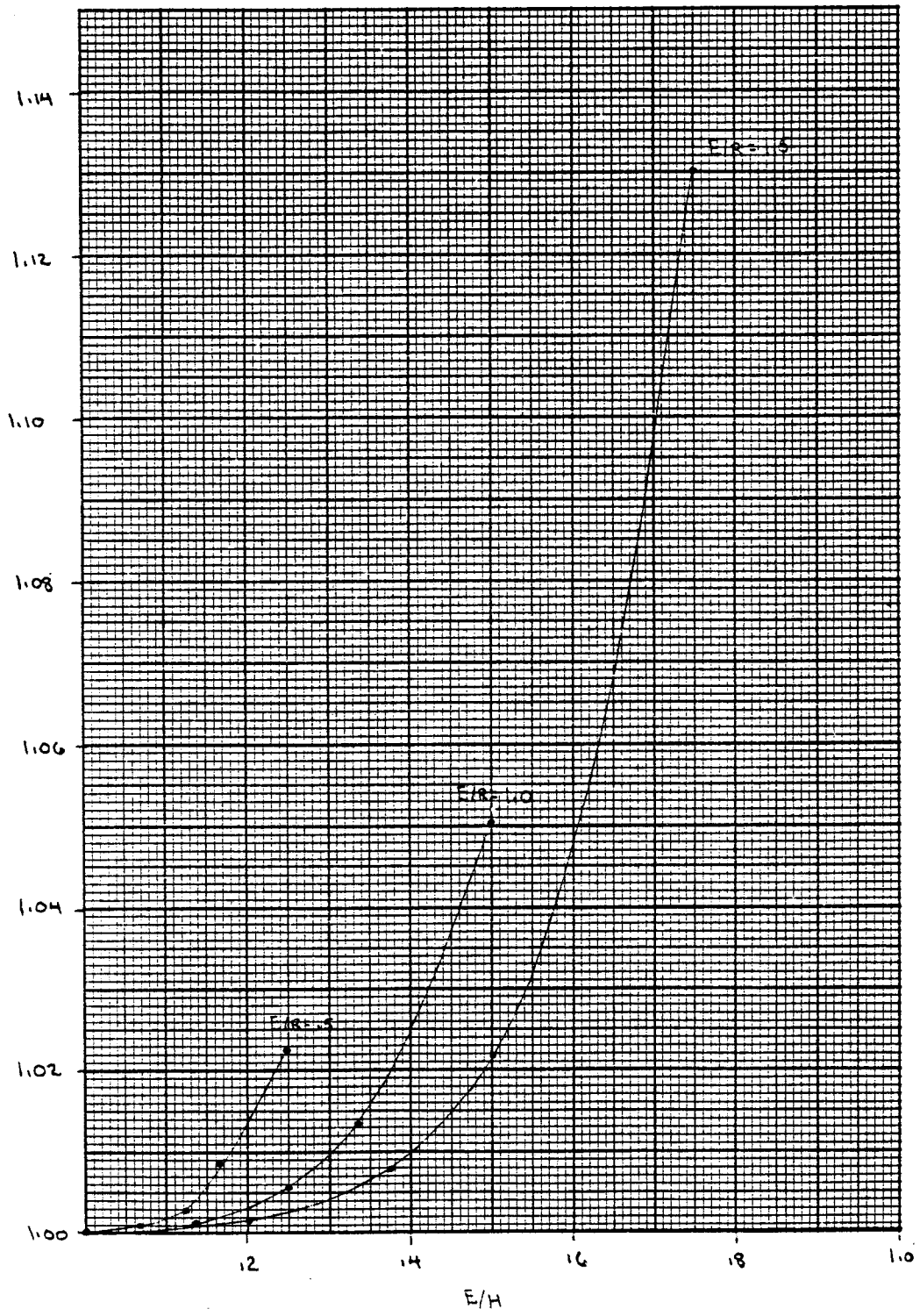

FIGURE 18

NORMALIZED TORSIONAL STIFFNESS $h(E/H) = \frac{K(R/H,\ E/R)}{K(R/H,\ E/R=0)} \div \frac{K(R/H=0,\ E/R)}{K(R/H=0,\ E/R=0)}$

VERSUS $\frac{E/H}{1 - E/H}$

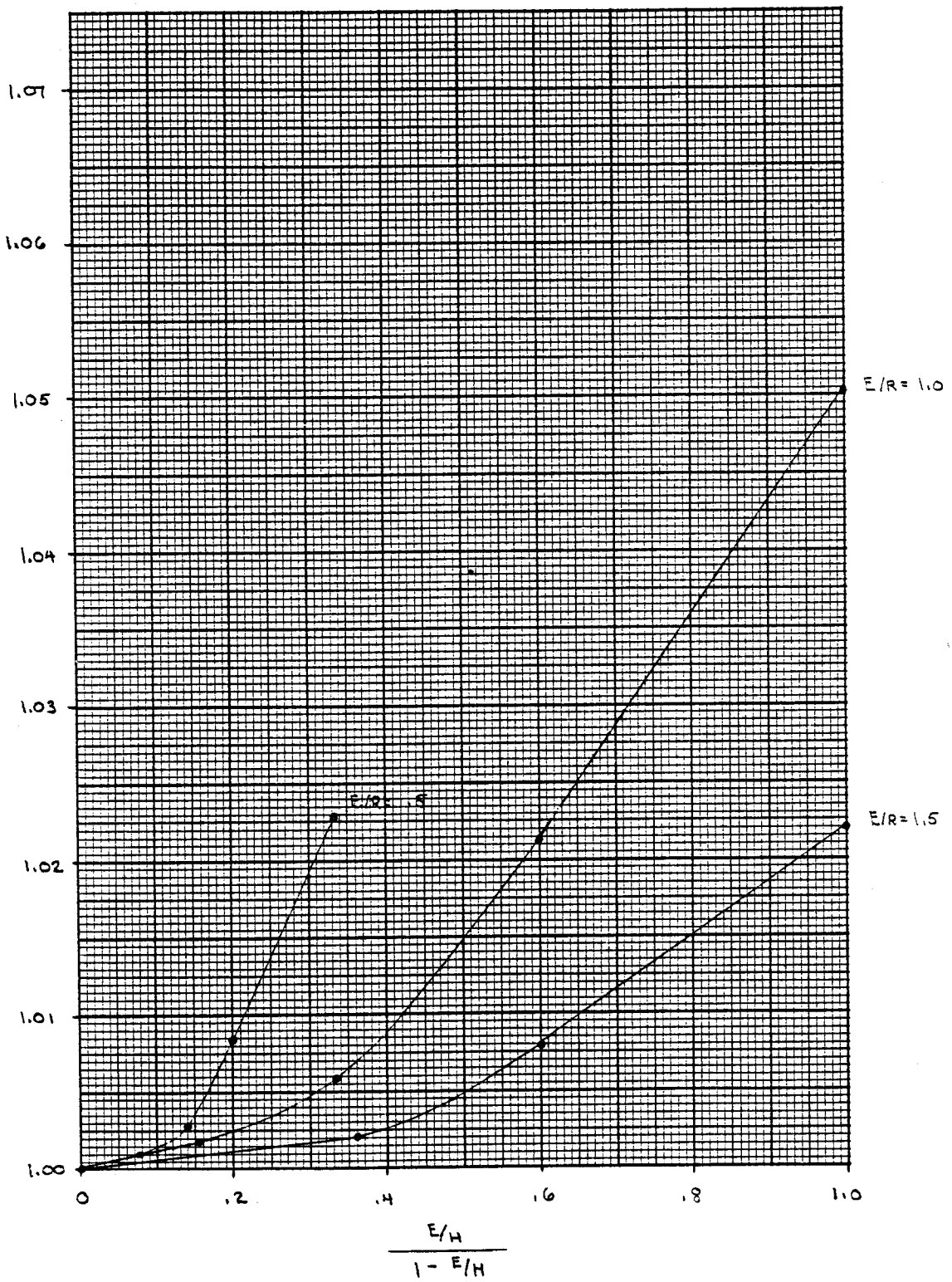

FIGURE 19

Table 8

E/R	H/R	E/H	$\frac{E/H}{1 - E/H}$	h(E/H)
0	2	0	0	1
	2	0	0	1
	4	0	0	1
	7.5	0	0	1
.5	2	.2000	.3333	1.0230
	3	.1667	.2000	1.0084
	4	.1250	.1424	1.0027
	7.5	.0667	.0715	1.0008
1.0	2	.5000	1.0000	1.0505
	3	.3333	0.5000	1.0136
	4	.2500	0.3333	1.0059
	7.5	.1333	0.1538	1.0017
1.5	2	.7500	3.0000	1.1303
	3	.5000	1.0000	1.0221
	4	.3750	0.6000	1.0080
	7.5	.2000	0.3600	1.0022

$$K_t = \frac{16GR^2}{3}(1 + 2.67\ E/R) \qquad (15)$$

Table 9 gives a comparison between the values of K_t computed using equation (15) and the original data by the finite element procedure. For the majority of the cases studied, the relative error is 5% or less, while the largest error is about 12%. The basic conclusion from this study is that the effects of strata depth on the static torsional stiffness of an embedded, cylindrical foundation are negligible. On the other hand, the stiffness is strongly dependent on the depth of embedment, but this increase is contingent upon the assumption of perfect weldment of the lateral walls to the surrounding soil.

Table 9

E/R	H/R	"EXACT"	EQUATION 15	ERROR %
0	2	5.37	5.33	.7
	3	5.34	5.33	.1
	4	5.33	5.33	-.1
	7.5	5.32	5.33	-.2
0.5	2	13.49	12.45	8.3
	3	13.24	12.45	6.3
	4	13.14	12.45	5.5
	7.5	13.09	12.45	5.1
1.0	2	20.94	19.57	7.0
	3	20.09	19.57	2.6
	4	19.90	19.57	1.7
	7.5	19.78	19.57	1.1
1.5	2	29.95	26.69	12.2
	3	26.93	26.69	.9
	4	26.51	26.69	- .7
	7.5	26.31	26.69	-1.4

6. DYNAMIC STIFFNESSES COEFFICIENTS

For dynamic, harmonic loads on elastic systems, forces and displacements are not in phase with each other, implying that the dynamic stiffness is a complex number. In the case of harmonically excited foundations, it is customary to express the dynamic stiffnesses (or impedance) K as

$$K = K^{\circ} (k + i\, a_o c)(1 + 2i\beta)$$

where K° is the static stiffness, and k, c are dimensionless functions referred to as stiffness coefficients; also, $a_o = \Omega R/C_s$ is the dimensionless frequency (with Ω = the excitation frequency, R = radius of the cylindric foundation, and C_s = shear wave velocity of the soil); and β = the material (hysteretic) damping of the soil.

COMPARISON BETWEEN THE "EXACT" FINITE ELEMENT VALUES AND EQUATION 15

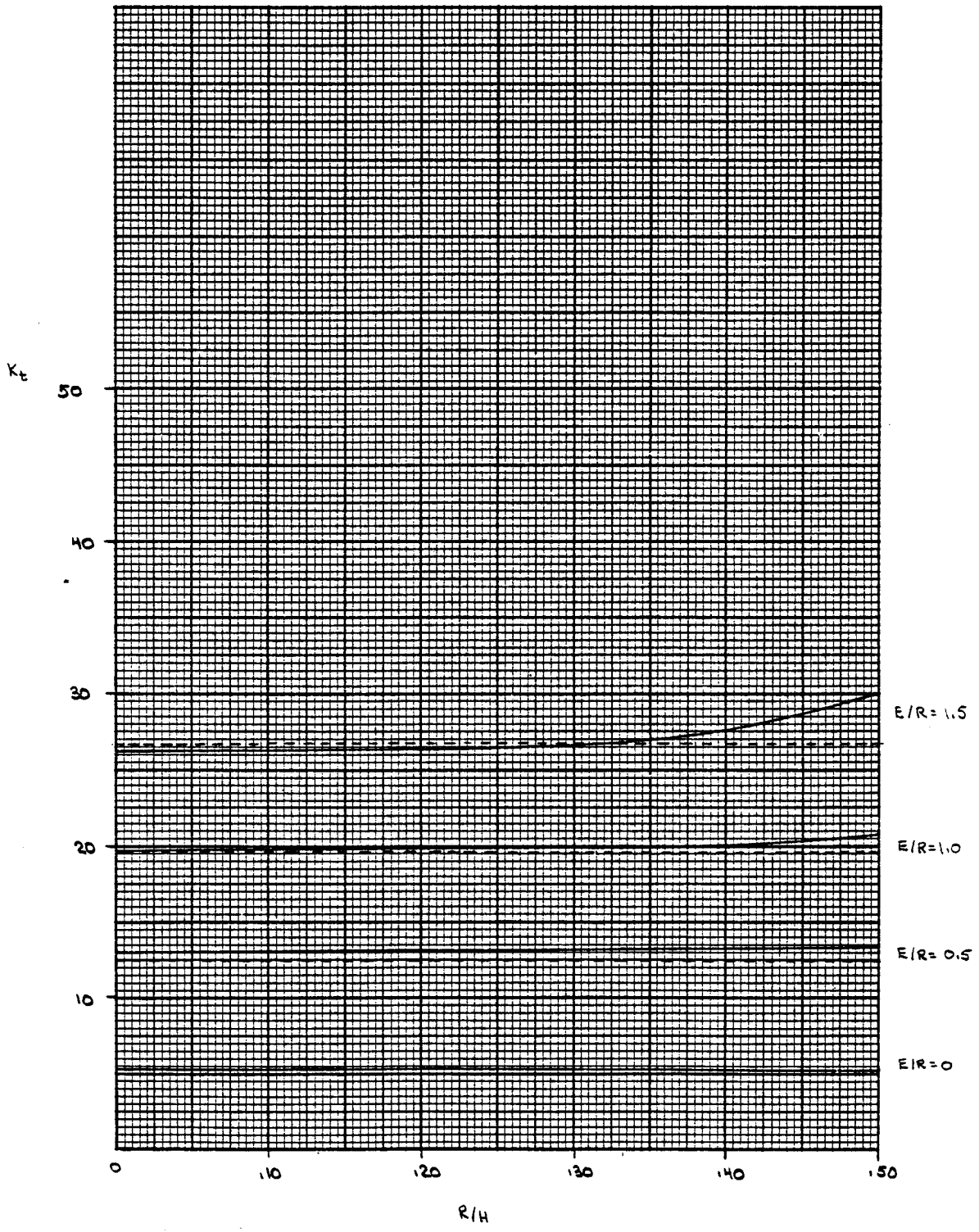

FIGURE 20

In general, k, c are functions of both frequency (a_0) and material damping (β), but in practical cases, the dependence of these functions on β is usually neglected. Nevertheless, this effect could be accounted for via the correspondence principle, if need should arise.

The computation of the dynamic stiffness functions for the vertical and torsional modes of vibration of a cylindric footing embedded in an elastic stratum was performed in this study with the finite element program referenced earlier. The cases analyzed are indicated in Table 10.

Table 10 - Foundation Geometry for Dynamic Case
ν = 0.333, regular mesh

H/R	E/R	β
2	0	.05, 0.10, 0.20
	1	.05, 0.10, 0.20
3	0	.05
	1	.05

In each case, a regular mesh (as shown in Fig. 1) was used, having square elements of size 1/4 × 1/4. It follows that the shortest wavelength λ that may be transmitted is about one radius, corresponding to a frequency $f_o = \lambda/C_s = 1$ ($a_o = 2\pi f_o = 2\pi$). Reasonably accurate results can then be expected for frequencies less than about half this maximum, i.e., $f_o < 0.5$.

It is well known that the coefficient c is related to the loss of energy to the system as a result of travelling waves. This effect is referred to as radiation damping. For a lossless medium (no material damping), there is no radiation damping below the fundamental dilatational frequency of the stratum for the vertical case, or below the fundamental shear beam frequency of the stratum for torsion. These frequencies are given, for a uniform stratum, by $C_p/4H$ and $C_s/4H$, respectively, with C_p, C_s being the dilatational and shear wave velocities of the soil, and H being the depth of the stratum. For a dissipative medium, on the other hand, there will be some radiation below these critical frequencies, the amount being a function of the material damping present. Low and high frequency ranges will, therefore, be studied separately.

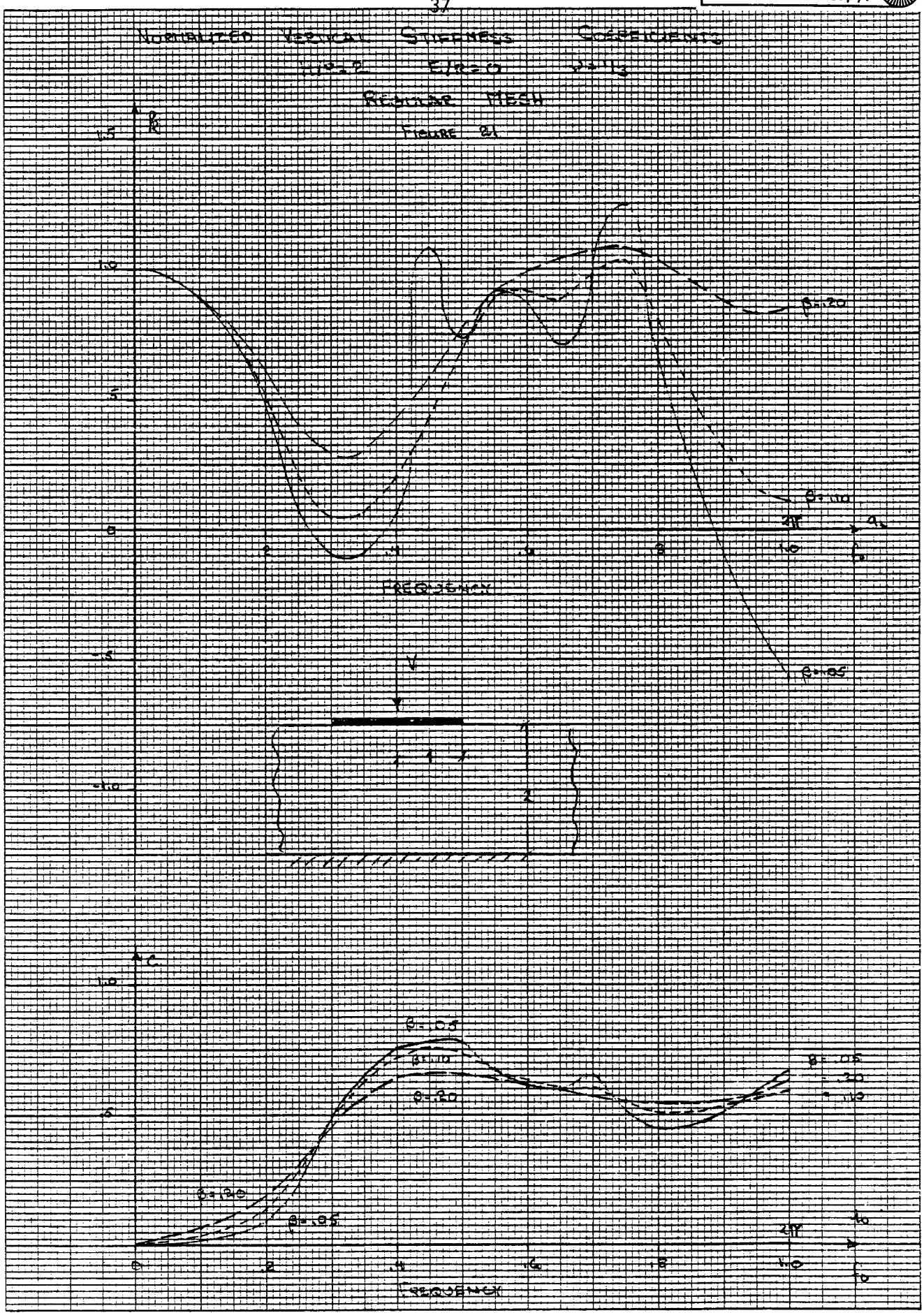

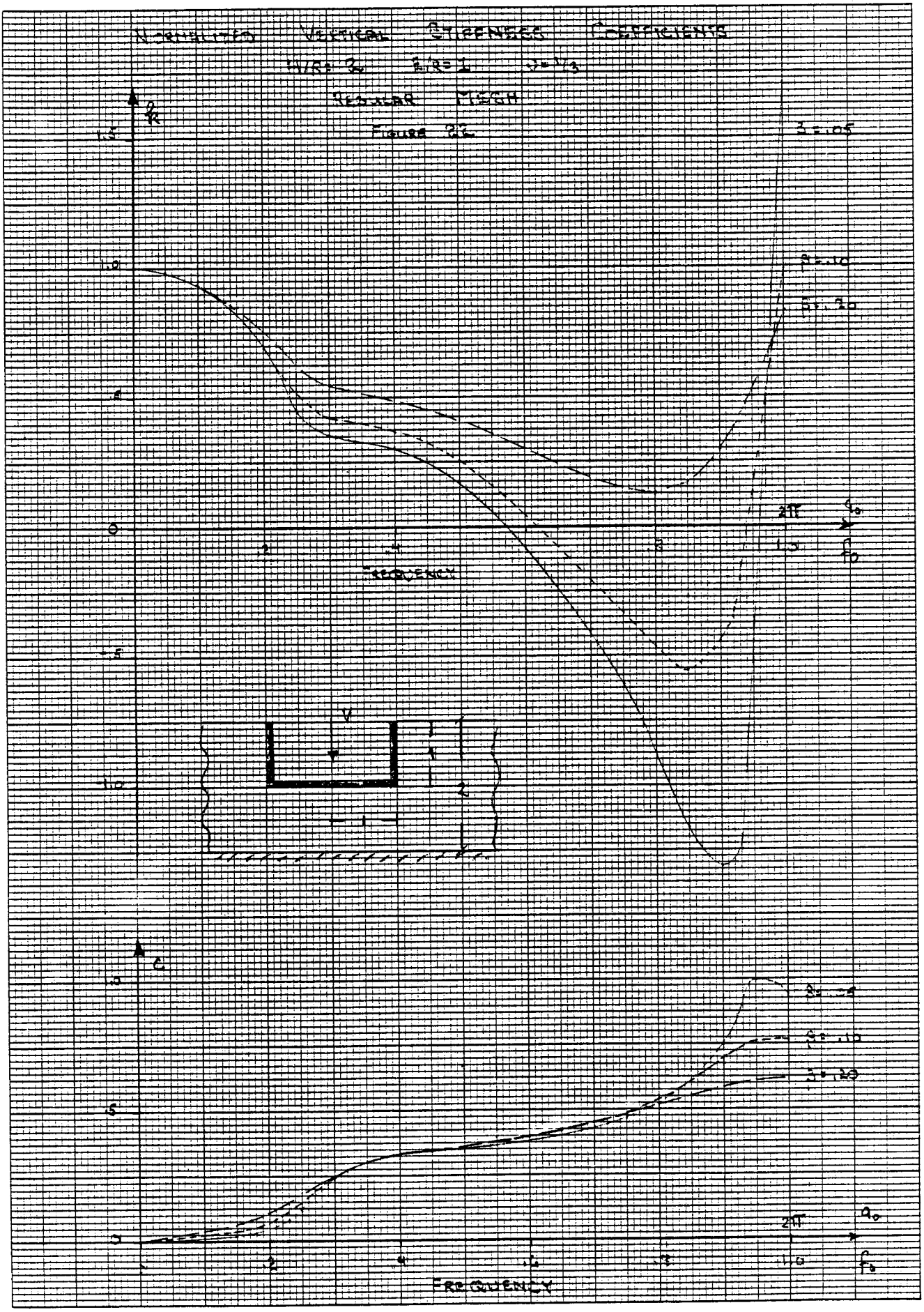
NORMALIZED VERTICAL STIFFNESS COEFFICIENTS
W/R= 3 r/R= 1/2 ν= 1/3
REGULAR MESH
FIGURE 22
k/k
1.5
1.0
.5
0
-.5
-1.0
ζ=.05
β=.10
β=.20
2π
a₀
b₀
FREQUENCY
V
1
1
2
1
c/c
1.0
.5
0
β=0
β=.10
β=.20
2π
a₀
b₀
FREQUENCY

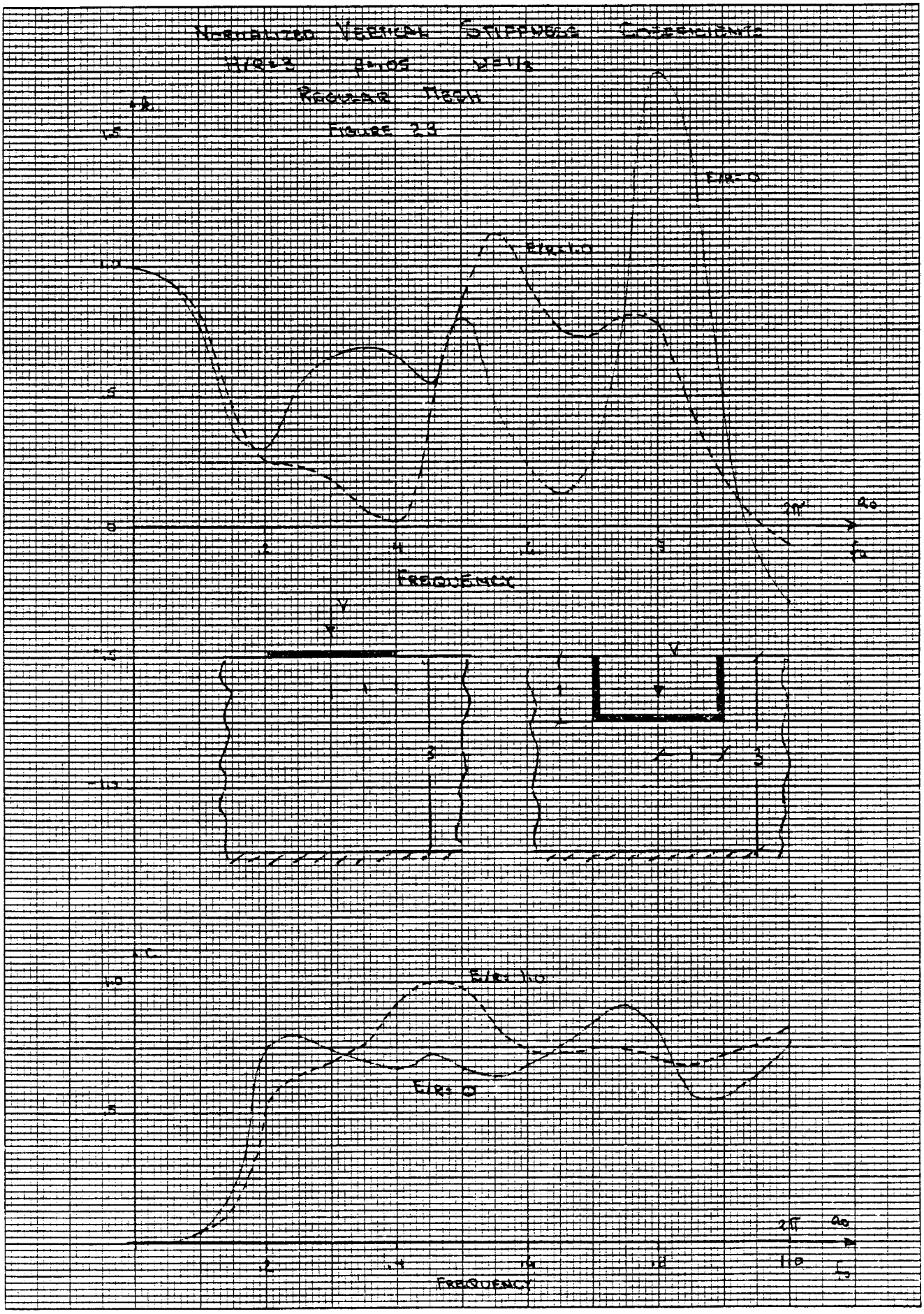
NORMALIZED VERTICAL STIFFNESS COEFFICIENTS
SIDE-2 B=.05 ν=1/2
REGULAR FLOW
FIGURE 23
E/R=0
E/R=1.0
FREQUENCY
V
E/R=1.0
E/R=0
FREQUENCY

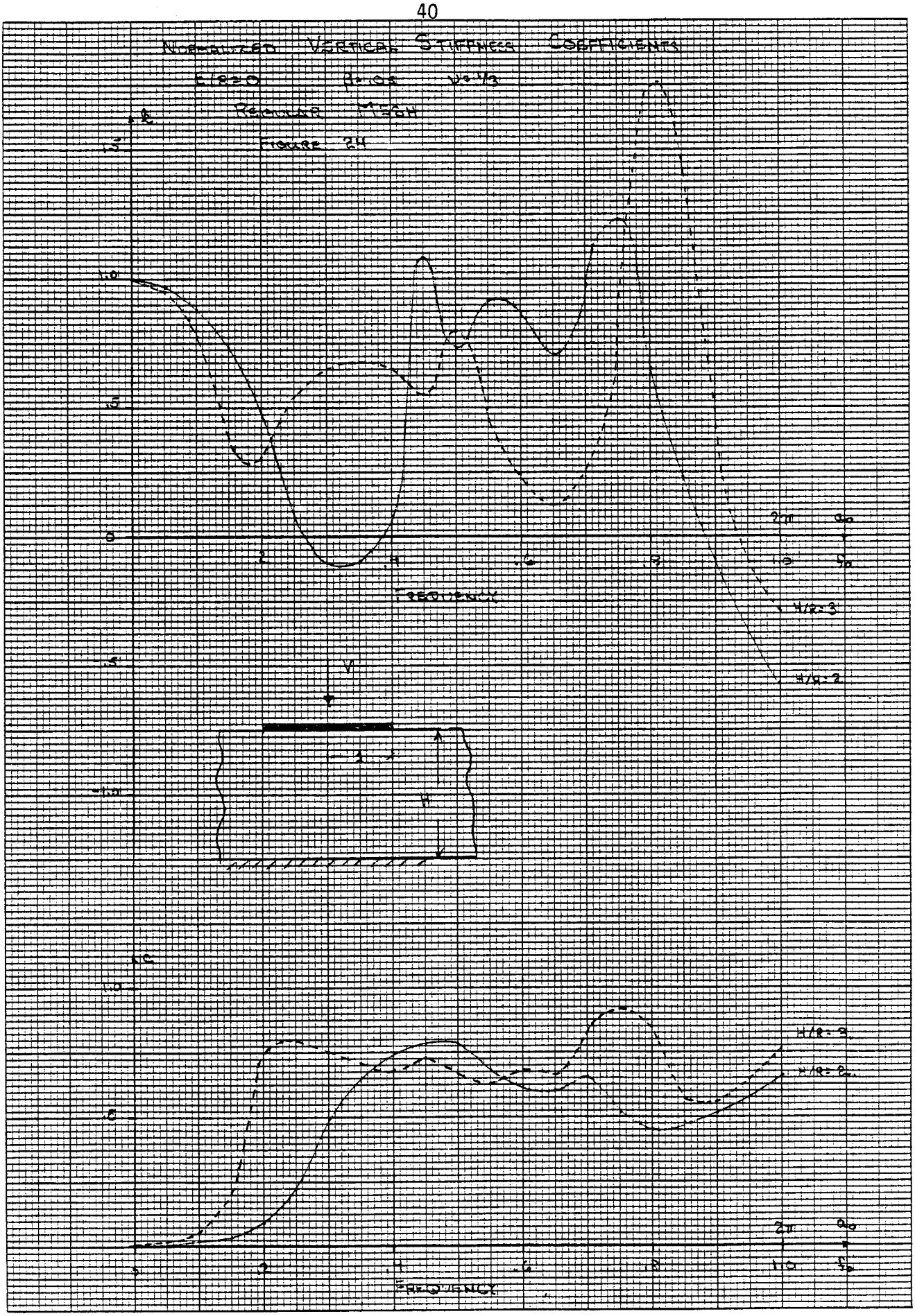
NORMALIZED VERTICAL STIFFNESS COEFFICIENTS
E/R=0
β=.05
ν=1/3
RECTANGULAR
MAT
FIGURE 24
K
1.5
1.0
.5
0
-.5
-1.0
FREQUENCY
V
H
H/R=3
H/R=2
KC
1.0
.5
0
FREQUENCY
H/R=3
H/R=2

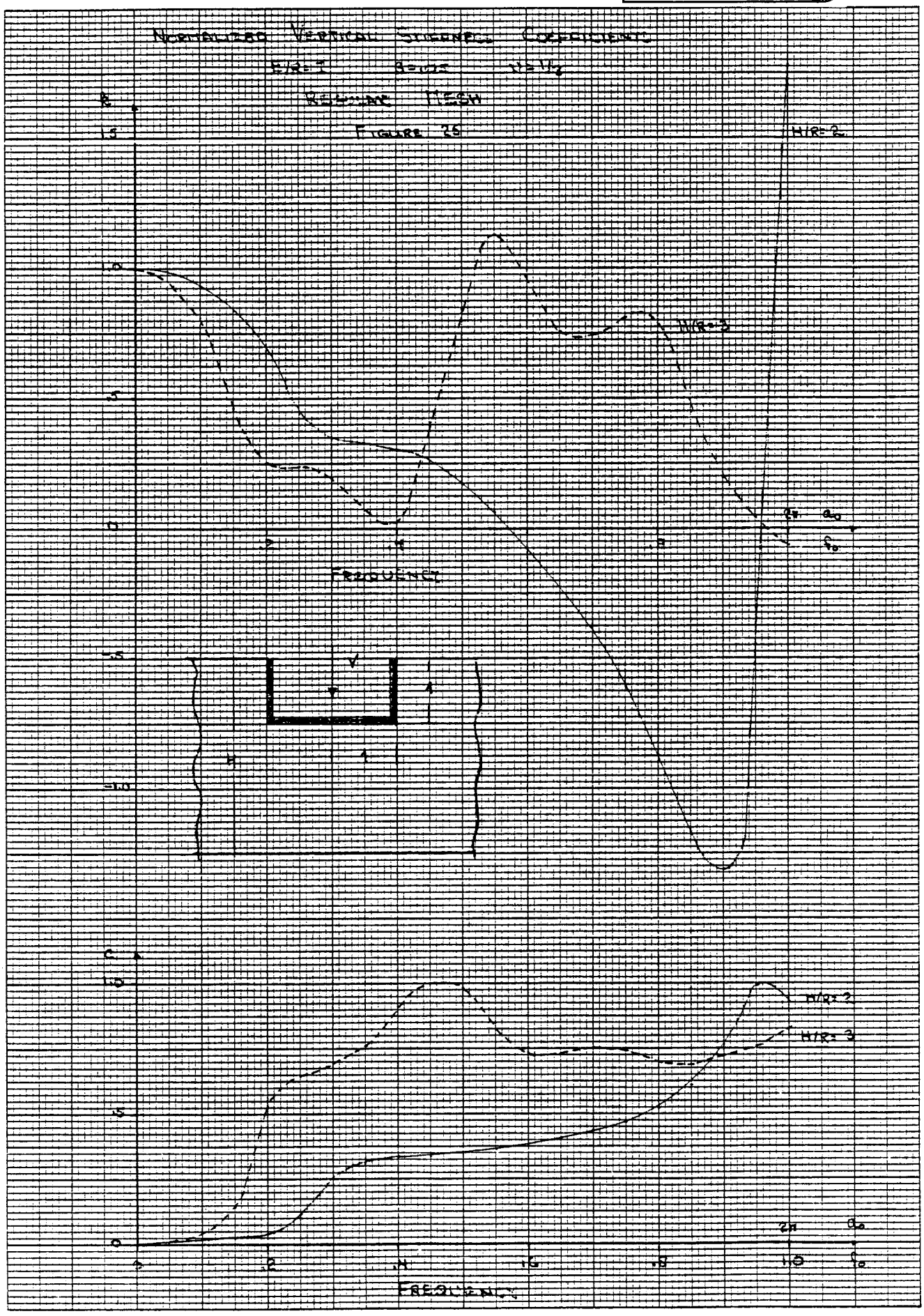

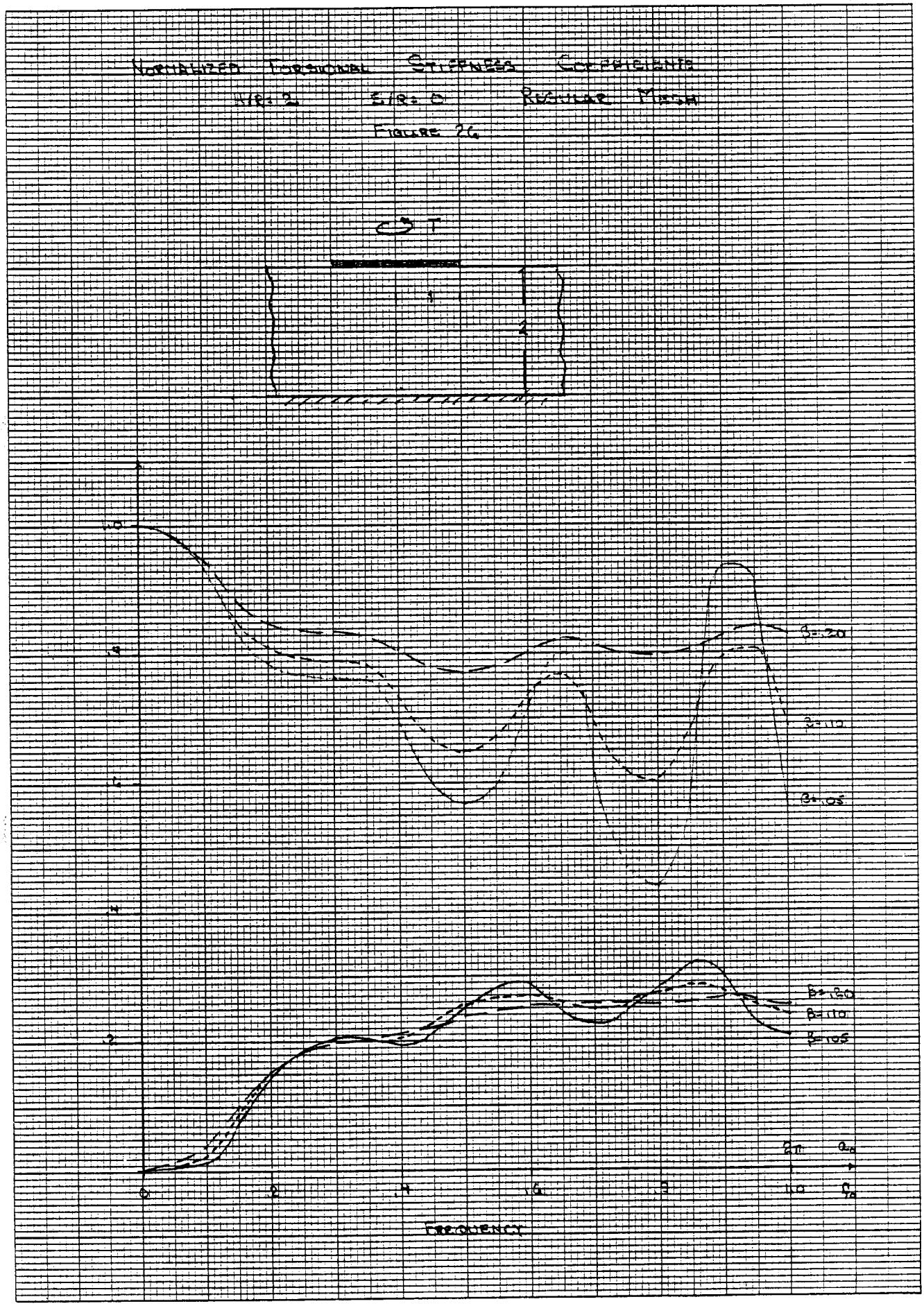
NORMALIZED TORSIONAL STIFFNESS COEFFICIENTS
R/B: 2 S/R: 0 REGULAR MODE
FIGURE 24
T
1
2
1.0
.8
.6
.4
.2
0
.2
.4
.6
.8
1.0
β=.20
β=.110
β=.105
β=.20
β=.110
β=.105
2π
a₀
1.0
f₀
FREQUENCY

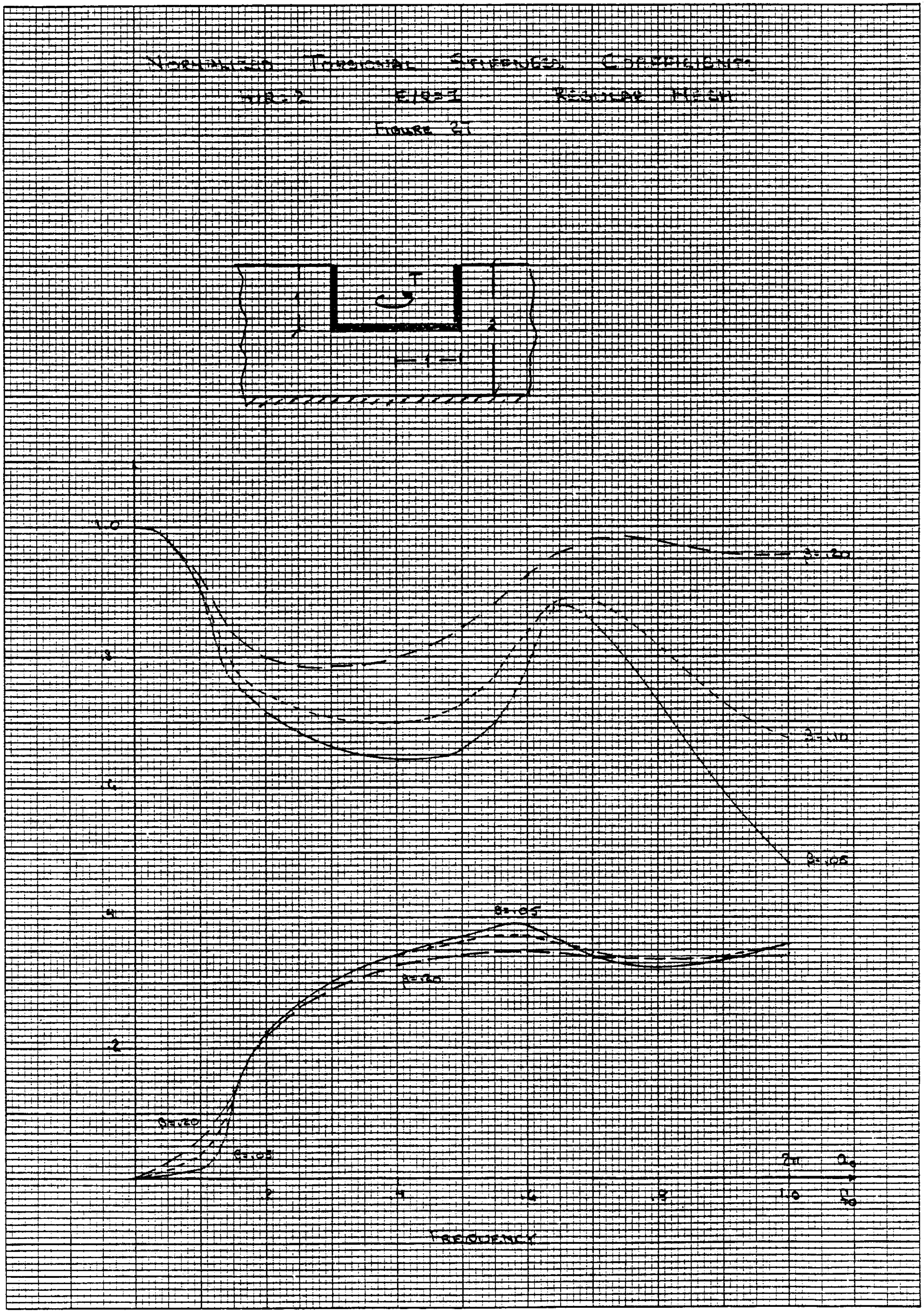
Normalized Torsional Stiffness Coefficient
Figure 27
T
1.0
.8
.6
.4
.2
β=.20
β=.10
β=.05
β=.05
β=.20
β=.20
β=.05
.2
.4
.6
.8
1.0
Frequency

NORMALIZED TORSIONAL STIFFNESS COEFFICIENTS

H/R= 3 β=.05 RIGID BAR MODE

FIGURE 28

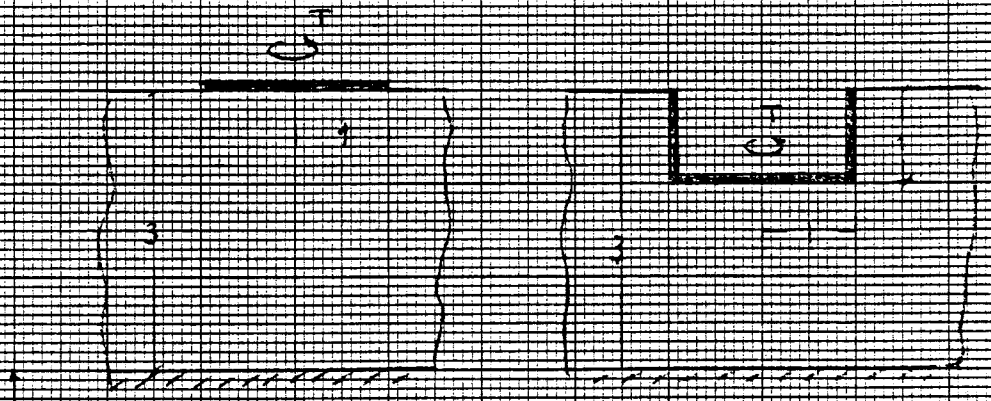

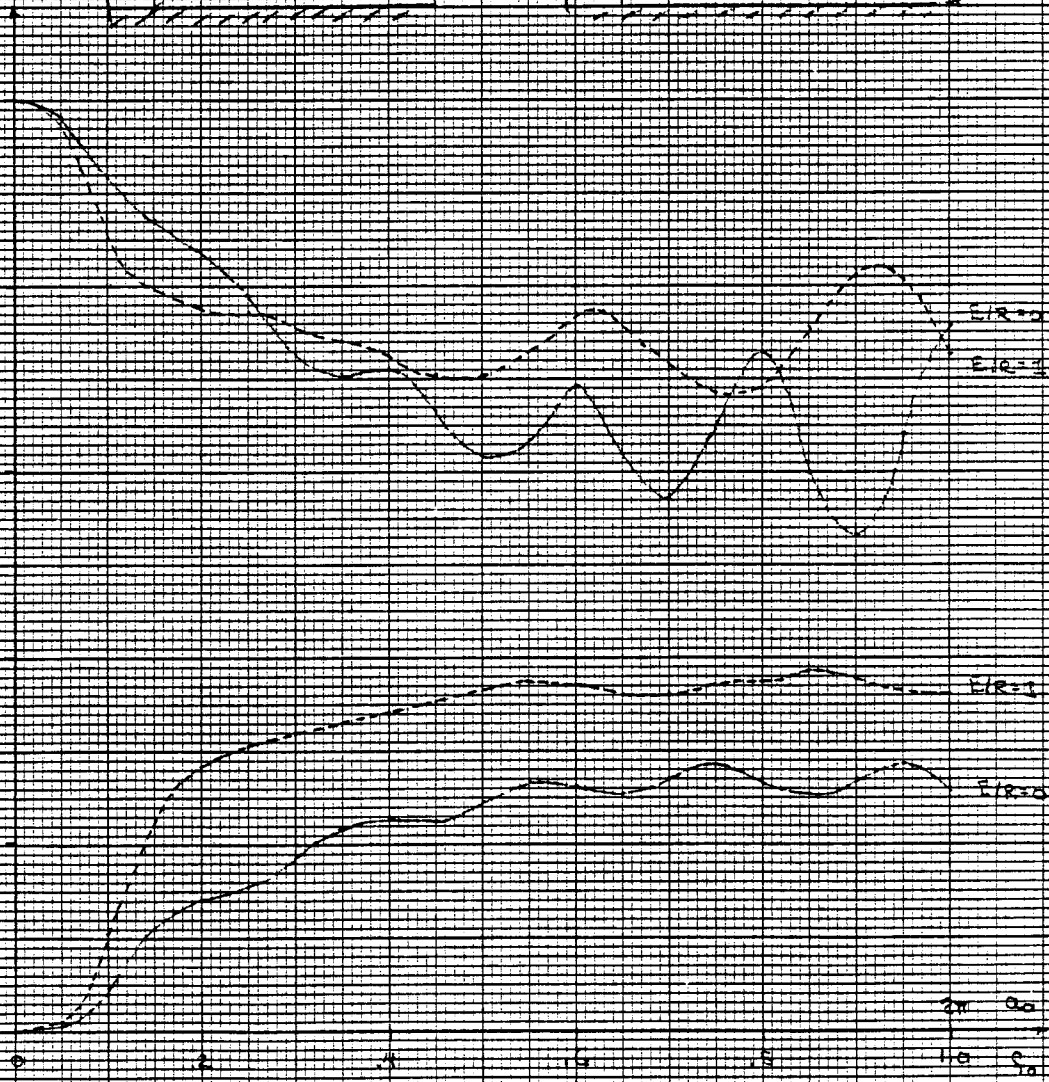

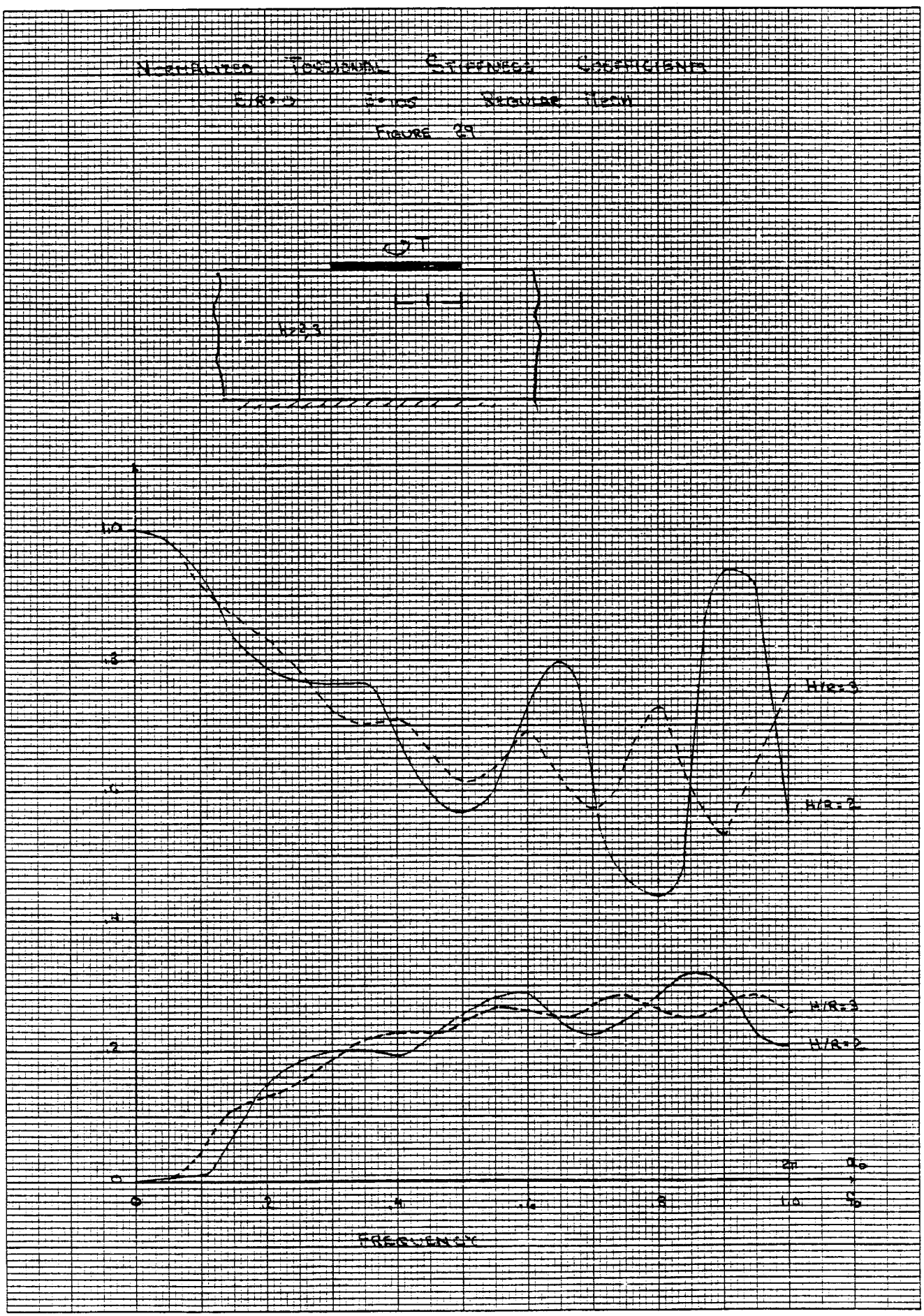
NORMALIZED TORSIONAL STIFFNESS COEFFICIENT
E/R=3 ν=.25 SQUARE PLATE
FIGURE 29
T
L
H/R=3
H/R=2
H/R=3
H/R=2
1.0
.8
.6
.4
.2
0
0
.2
.4
.6
.8
1.0
FREQUENCY

NORMALIZED TORSIONAL STIFFNESS COEFFICIENTS

E/R=3 β=1.25 RECTANGULAR TUBE

FIGURE 30

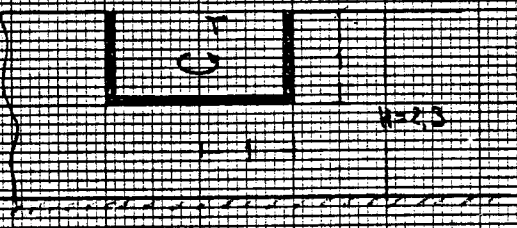

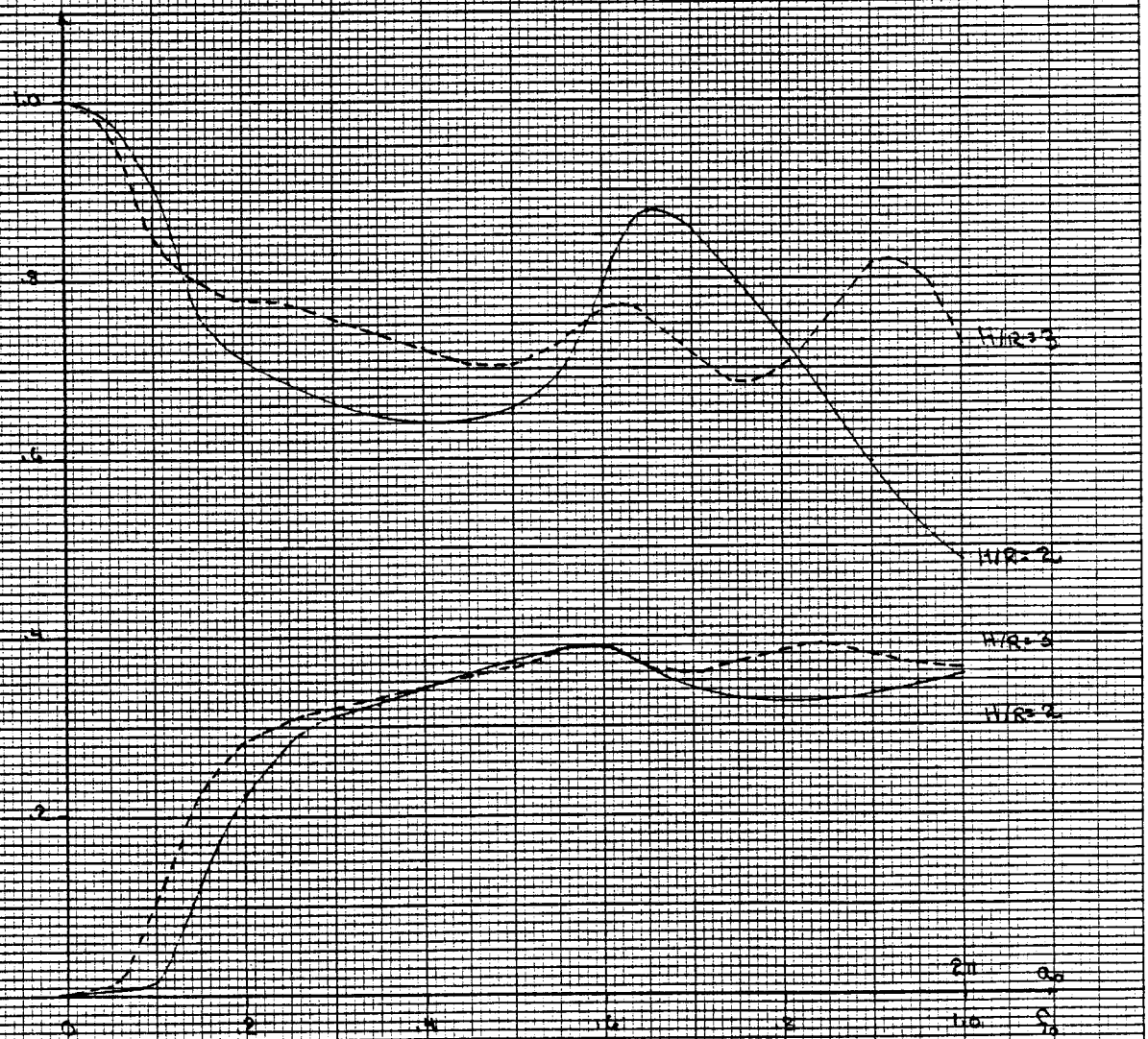

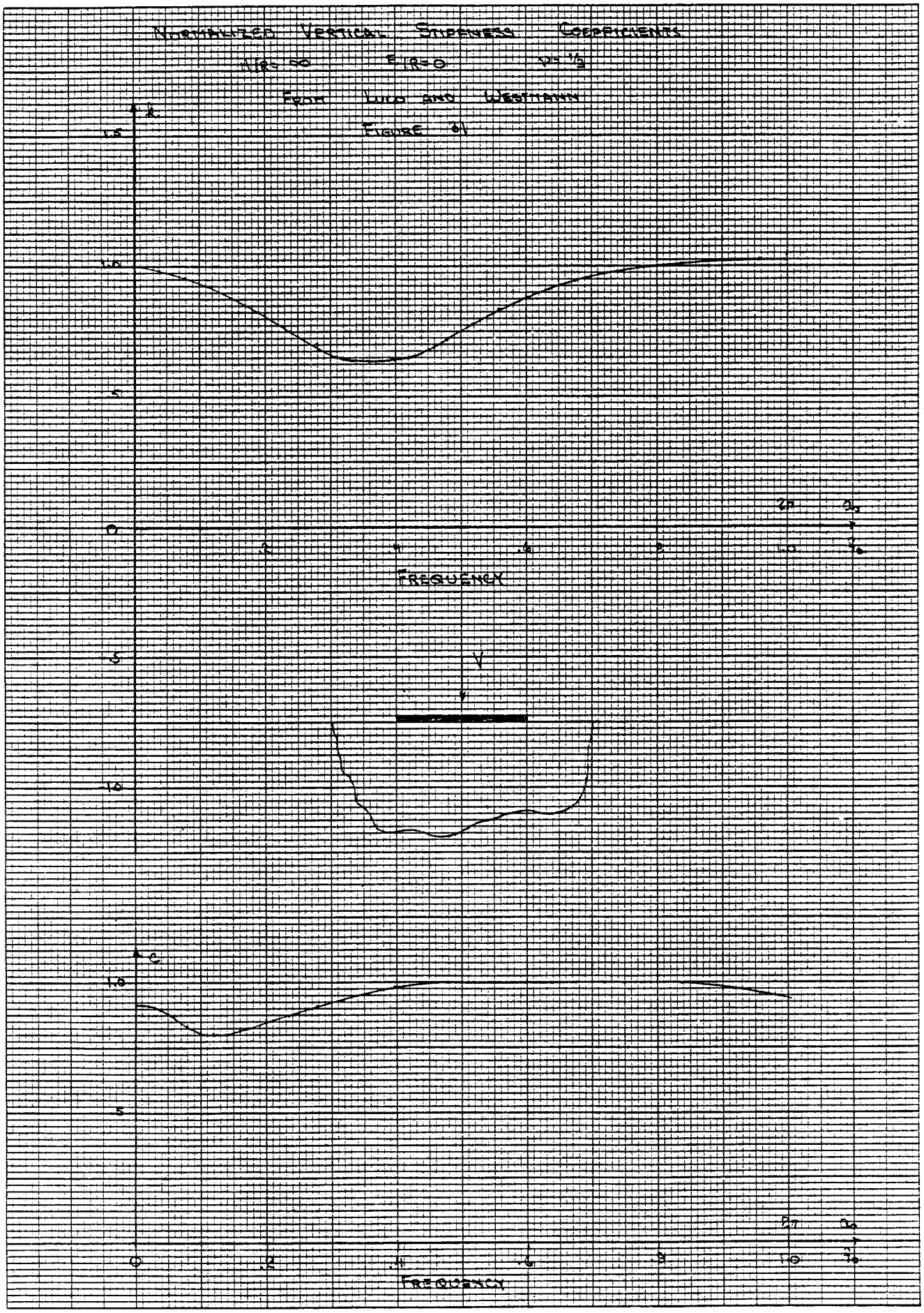

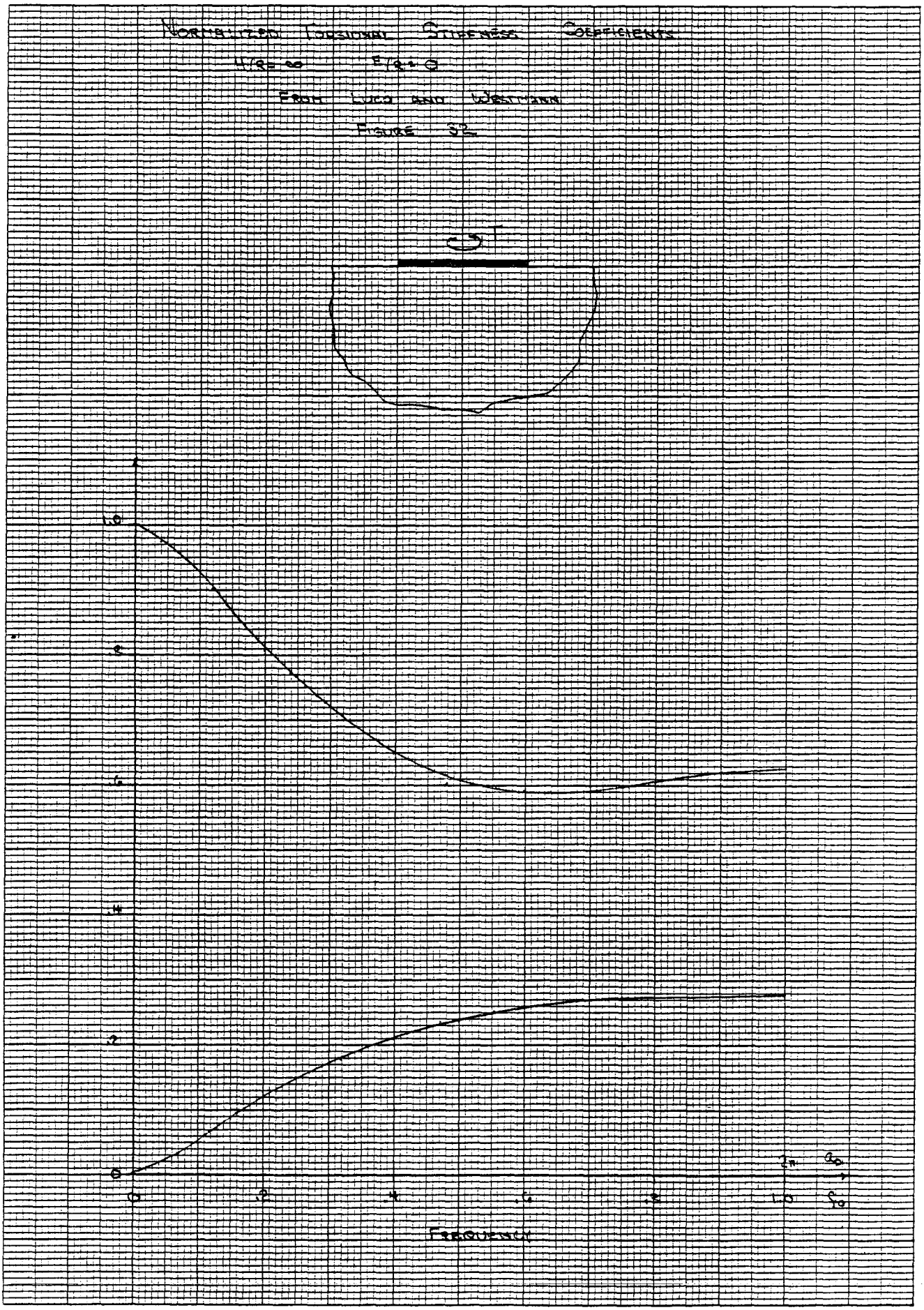
NORMALIZED TORSIONAL STIFFNESS COEFFICIENTS
H/R = ∞ E/G = 3
FROM LUCO AND WESTMANN
FIGURE 5B
CT
1.0
.8
.6
.4
.2
0
0
.2
.4
.6
.8
1.0
FREQUENCY

NORMALIZED TORSIONAL STIFFNESS COEFFICIENTS

W/R = ∞ E/R = 1/16

FROM ARSEL AND LUCO

FIGURE 33

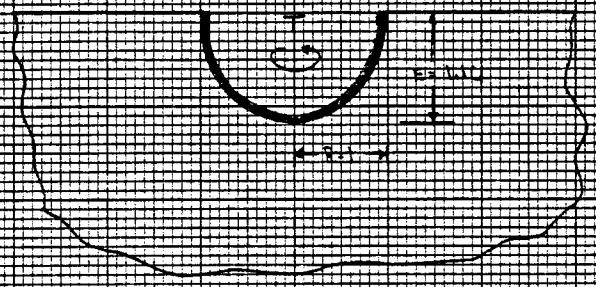

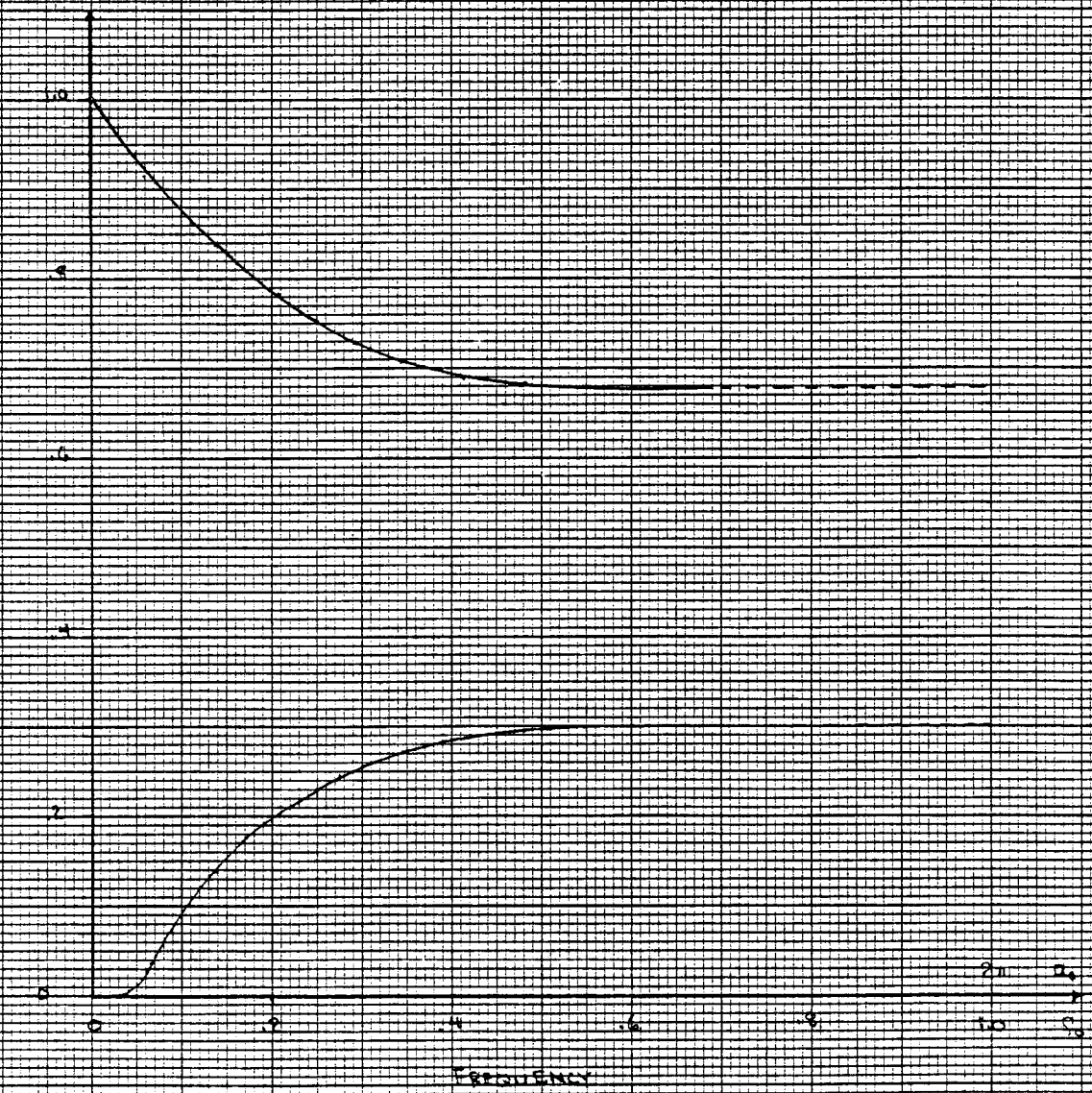

Figs. 21 through 25 show the stiffness coefficients for the vertical case, while Figs. 26 through 30 show these coefficients for torsion. Figs. 31 and 32 , on the other hand, depict the "exact" stiffness function derived by Luco (17) for a rigid disk over the surface of an elastic halfspace. Finally, Fig. 33 depicts the torsional stiffness coefficients for an ellipsoidal foundation embedded in an elastic halfspace, as reported by Apsel and Luco (2). The aspect ratio of the ellipsoid was chosen in such a way that the static torsional stiffness of the ellipsoid equals that of a cylindric foundation with E/R = 1.

It can be seen that both embedment and stratum depth have a marked influence on the dynamic stiffness coefficients, particularly for the vertical case. The real part (k) shows large variations and waviness as a result of wave reflections at the bottom boundary; this follows from the fact that for a lossless medium (β=0), the dynamic vertical stiffness vanishes at the dilatational frequencies of the stratum. The real part of the torsional stiffness, on the other hand, is more insensitive to embedment and stratum depth, and follows a trend similar to that of a surface circular plate on an elastic halfspace.

The imaginary parts for both the vertical and torsional case show, in general, much less waviness, following a trend similar to the imaginary parts corresponding to the problem of a disk in an elastic halfspace. Except for the case of a deep cylinder buried in a very shallow stratum (Figs.21, 22), embedment typically increases the amount of radiation, particularly in the torsional case.

In view of the above, it is probably reasonable (and conservative) to use the halfspace values in practical situations not requiring great sophistication, or when a computer program for the evaluation of the dynamic stiffnesses is not available.

Finally, Figs.34 through 41 show the imaginary parts of the stiffness functions in the low frequency range. As stated before, the amount of radiation is significantly less below the fundamental frequencies of the stratum, particularly for low values of internal damping. Following Elsabee (8) and Kausel et al. (13), empirical approximations are proposed of the form:

NORMALIZED VERTICAL STIFFNESS COEFFICIENT (IMAGINARY COEFFICIENT)

FINITE ELEMENT - "EXACT"

Frequency	H/R = 0						H/R = 3	
		E/R = 0			E/R = 1		E/R = 0	E/R = 1
	β = .05	.10	.20	.05	.10	.20	.05	.05
.0501	.008324	.01617	.02925	.005104	.009914	.01766	.01604	.01437
.1001	.01875	.03618	.06358	.01105	.02307	.03792	.05557	.04257
.1501	.04661	.07418	.1151	.02164	.03863	.06452	.2103	.1476
.2001	.09305	.1367	.1915	.04207	.06922	.1048	.7477	.5224
.2501	.2264	.2764	.3134	.1187	.1465	.1713	.7926	.6460

APPROXIMATE FORMULA

$$c = \frac{.67\ \beta\ \xi}{1 - (1-2\beta)\xi^2} \qquad \xi_p = f/f_p \leq 1 \qquad f_p = \frac{C_p}{4H}$$

Frequency	H/R = 2						H/R = 3	
		E/R = 0			E/R = 1		E/R = 0	E/R = 1
	β = .05	.10	.20	.05	.10	.20	.05	.05
.0501	.0069	.0138	.0274	.0069	.0138	.0274	.0109	.0109
.1001	.0156	.0306	.0593	.0156	.0306	.0593	.0296	.0296
.1501	.0296	.0562	.1021	.0296	.0562	.1021	.1112	.1112
.2001	.0630	.1095	.1734	.0630	.1095	.1734	.85	.85
.2501	.3359	.3345	.3339	.3359	.3345	.3339	.85	.85

TABLE 11

NORMALIZED VERTICAL STIFFNESS (IMAGINARY COMPONENT)

H/R=2 E/R=0 ν=1/3 REGULAR MESH

FIGURE 34

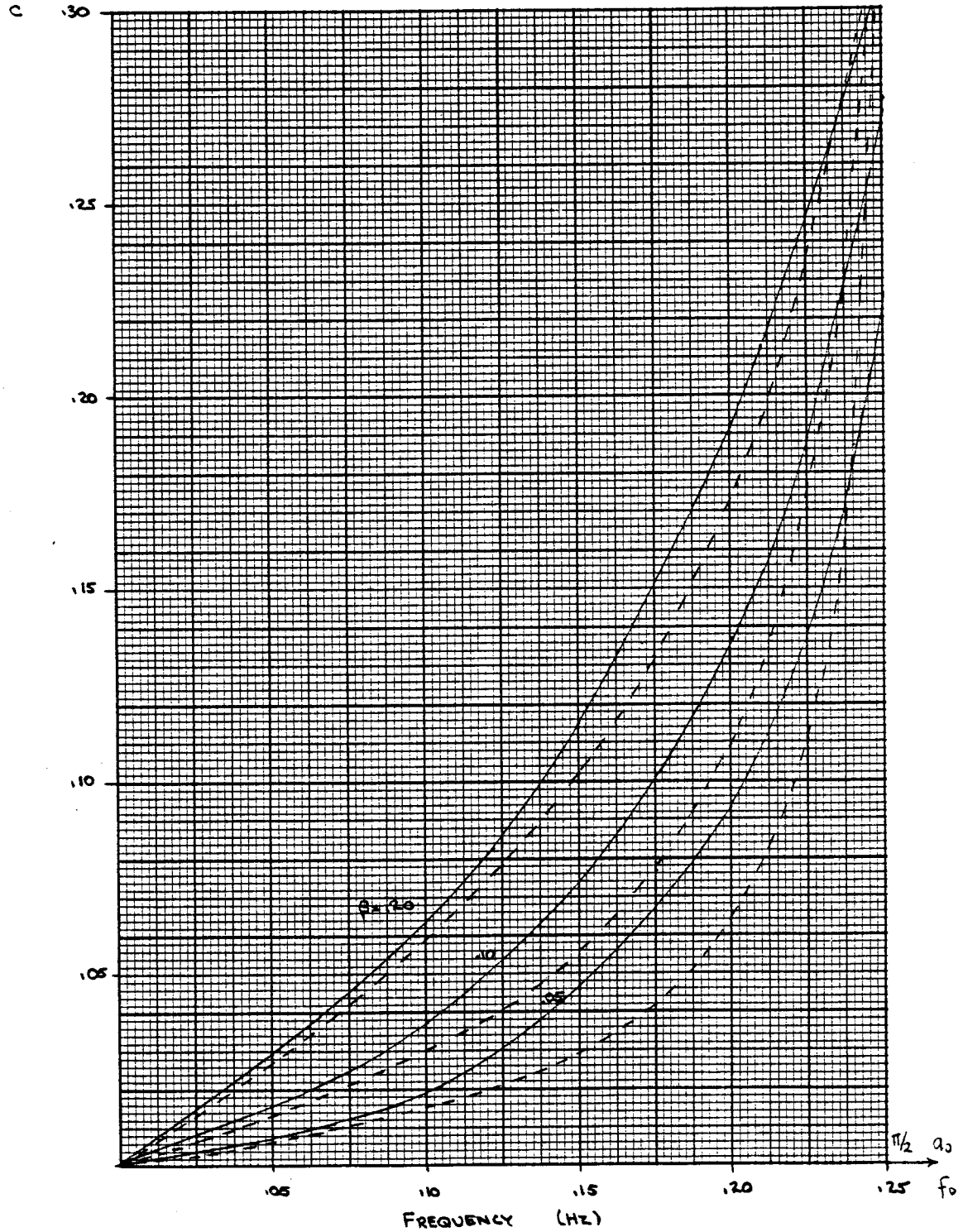

NORMALIZED VERTICAL STIFFNESS (IMAGINARY COMPONENT)

H/R=2 E/R=1 $\nu = 1/3$ REGULAR MESH

FIGURE 35

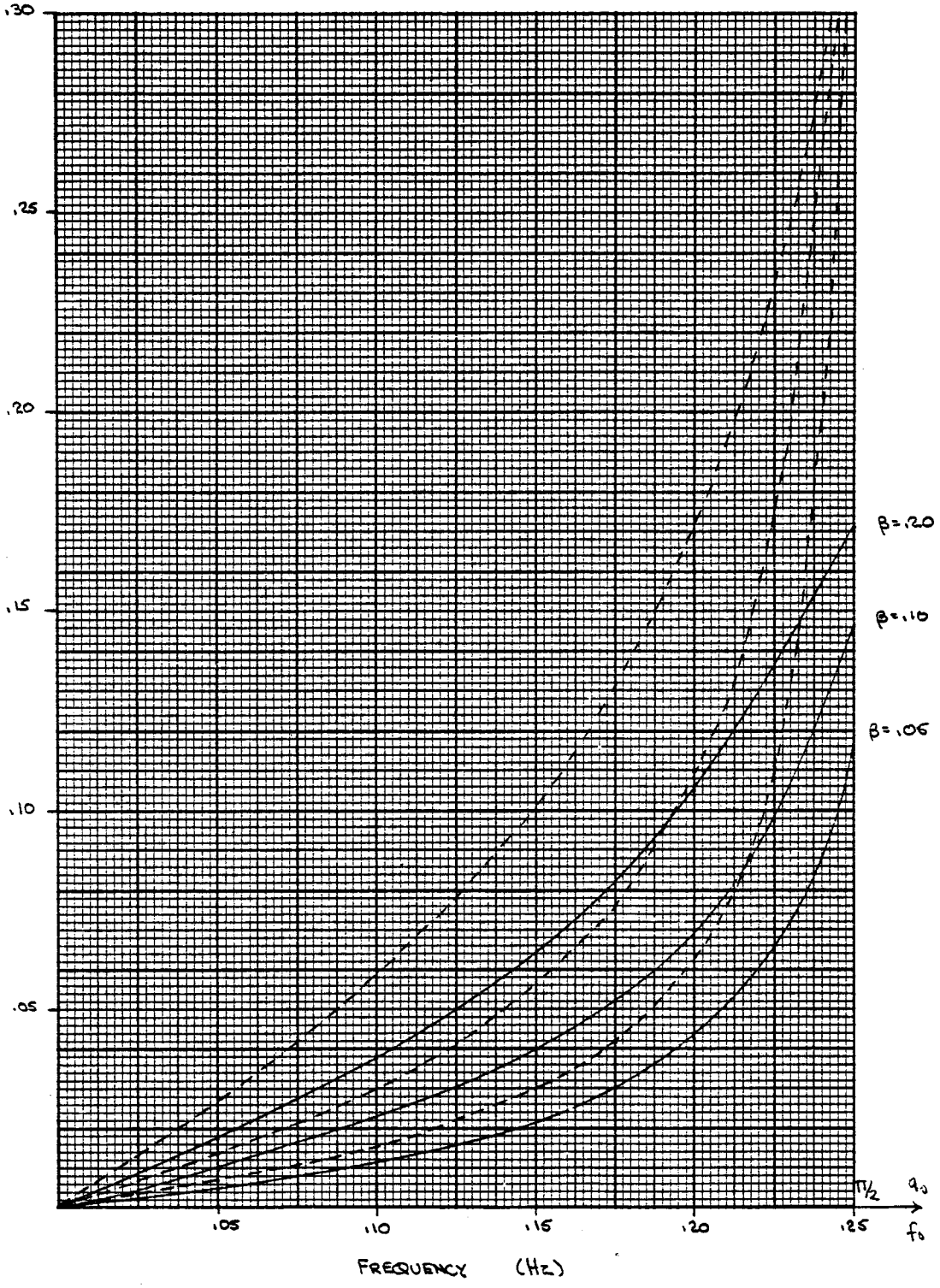

NORMALIZED VERTICAL STIFFNESS (IMAGINARY COMPONENT)

H/R= 2 β=.05 ν=1/3 REGULAR MESH

FIGURE 36

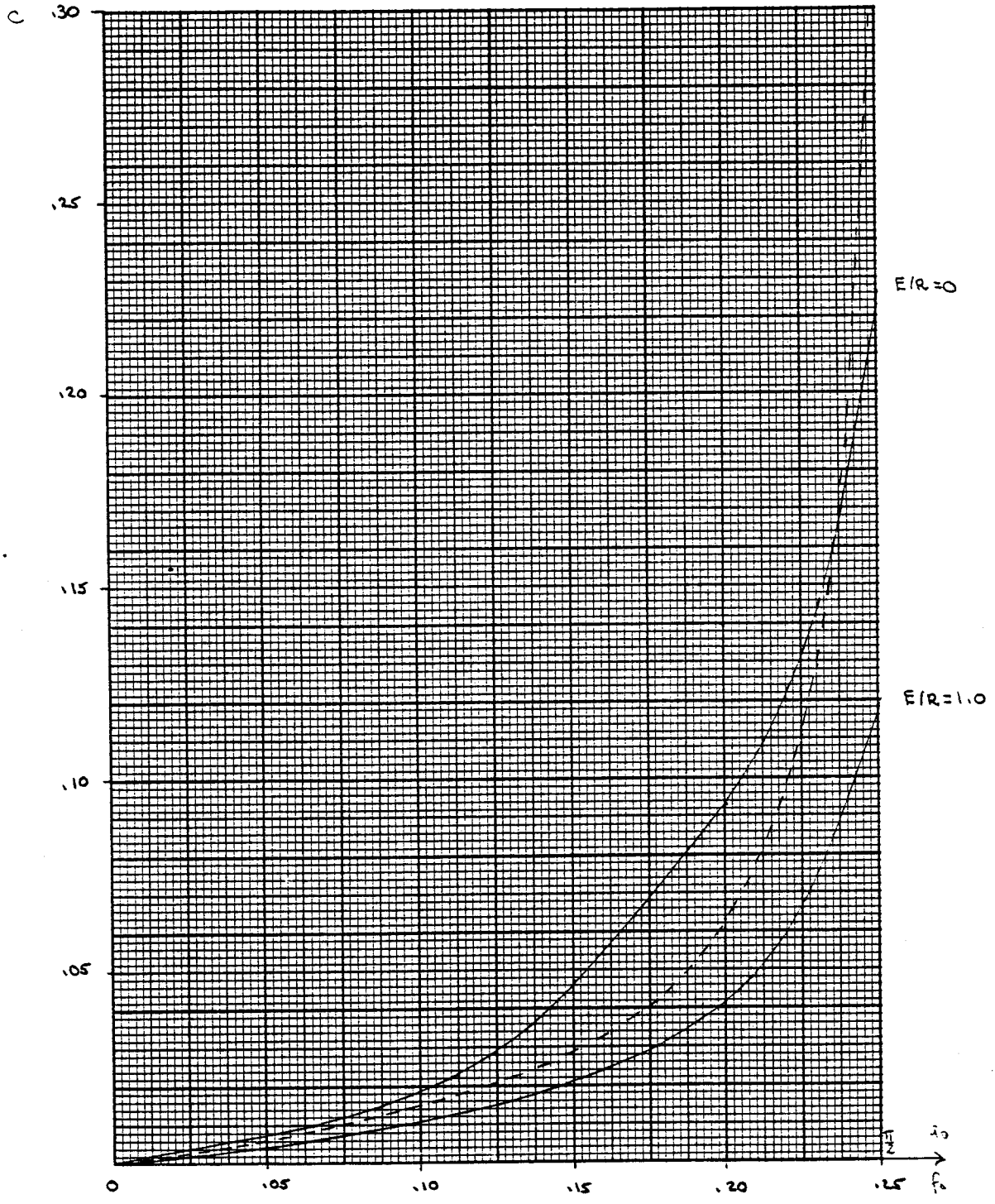

FREQUENCY (Hz)

NORMALIZED VERTICAL STIFFNESS (IMAGINARY COMPONENT)

H/R = 3 β = .05 ν = 1/3 REGULAR MESH

FIGURE 37

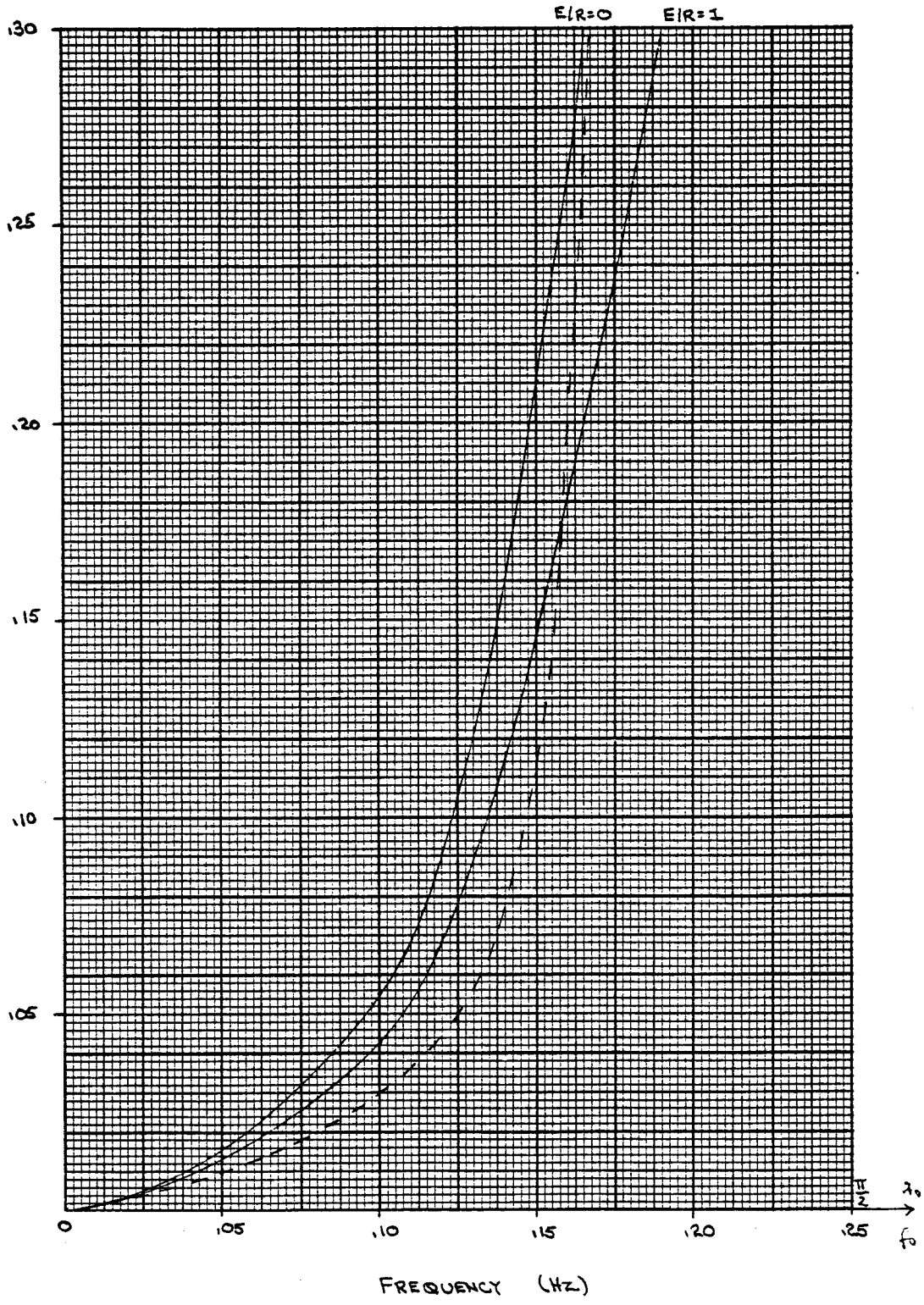

NORMALIZED TORSIONAL STIFFNESS COEFFICIENT (IMAGINARY COEFFICIENT)

FINITE ELEMENT - "EXACT"

Frequency	H/R = 2						H/R = 3	
	E/R = 0			E/R = 1			E/R=0	E/R=1
	β = .05	.10	.20	.05	.10	.20	.05	.05
.0501	.004744	.008810	.01580	.006770	.01315	.02307	.005830	.01028
.1001	.01230	.02352	.03989	.01827	.03477	.05837	.04832	.01044
.1501	.07916	.08679	.09481	.1260	.1346	.1425	.1123	.2288
.2001	.1496	.1512	.1490	.2236	.2249	.2196	.1422	.2847
.2501	.1874	.1866	.1804	.2723	.2721	.2630	.1532	.3084

APPROXIMATE FORMULA

$$C = \frac{0.15\beta\xi}{1 - (1-2\beta)\xi^2} \qquad \xi = f/f_s \leq 1 \qquad f_s = \frac{C_s}{4H}$$

Frequency	H/R = 2						H/R = 3	
	E/R = 0			E/R = 1			E/R=0	E/R=1
	β =.05	.10	.20	.05	.10	.20	.05	.05
.0501	.0035	.0069	.0133	.0035	.0069	.0133	.0067	.0067
.1001	.0142	.0247	.0390	.0142	.0247	.0390	.0495	.0495
.1501	.0923	.0923	.0923	.0923	.0923	.0923	.0923	.0923
.2001	.1324	.1324	.1324	.1324	.1324	.1324	.1324	.1324
.2501	.1658	.1658	.1658	.1658	.1658	.1658	.1658	.1658

TABLE 12

NORMALIZED TORSIONAL STIFFNESS (IMAGINARY COMPONENT)

H/R=2 E/R=0 REGULAR MESH

FIGURE 38

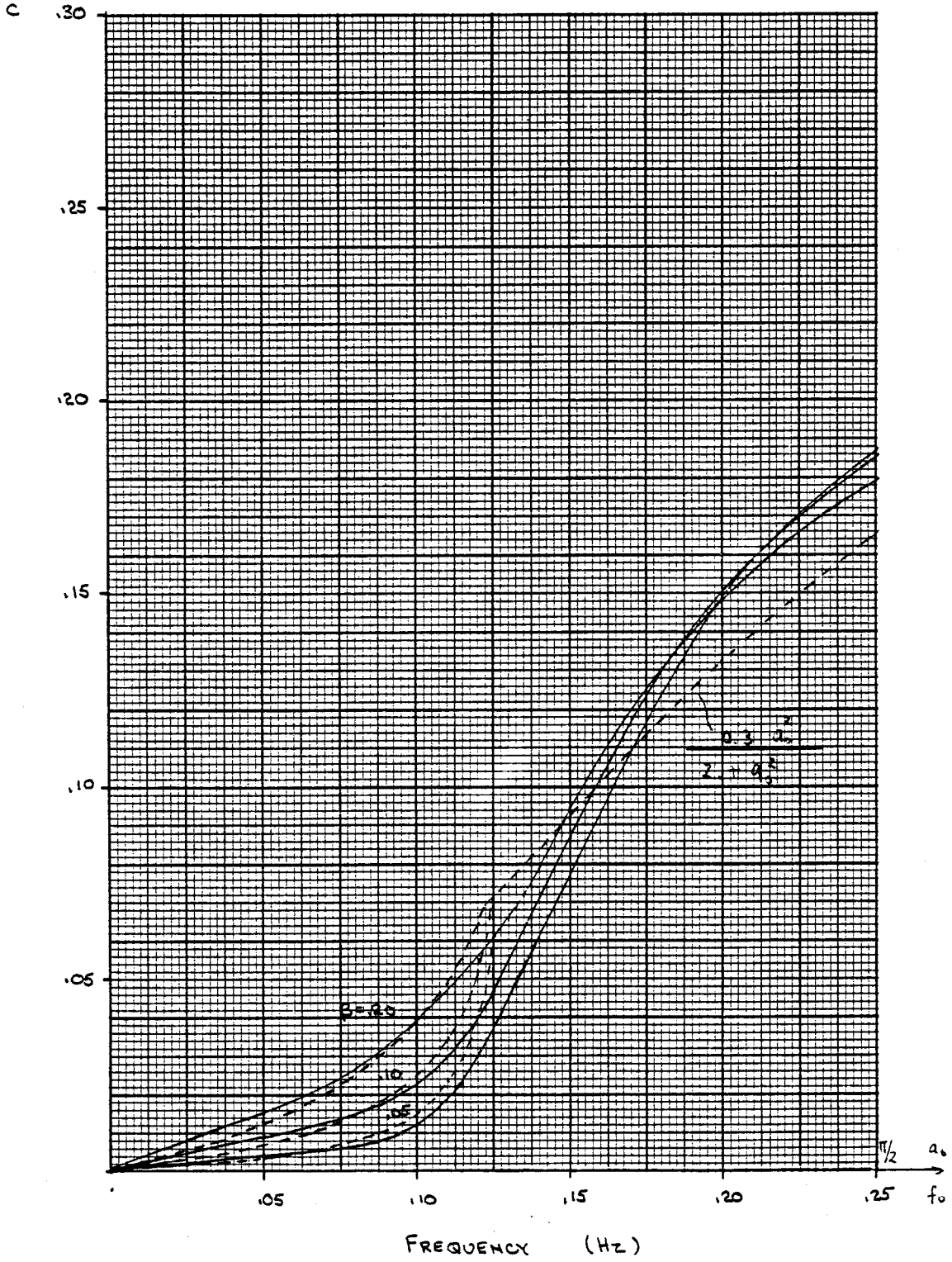

NORMALIZED TORSIONAL STIFFNESS (IMAGINARY COMPONENT)

H/R=2 E/R=1 REGULAR MESH

FIGURE 39

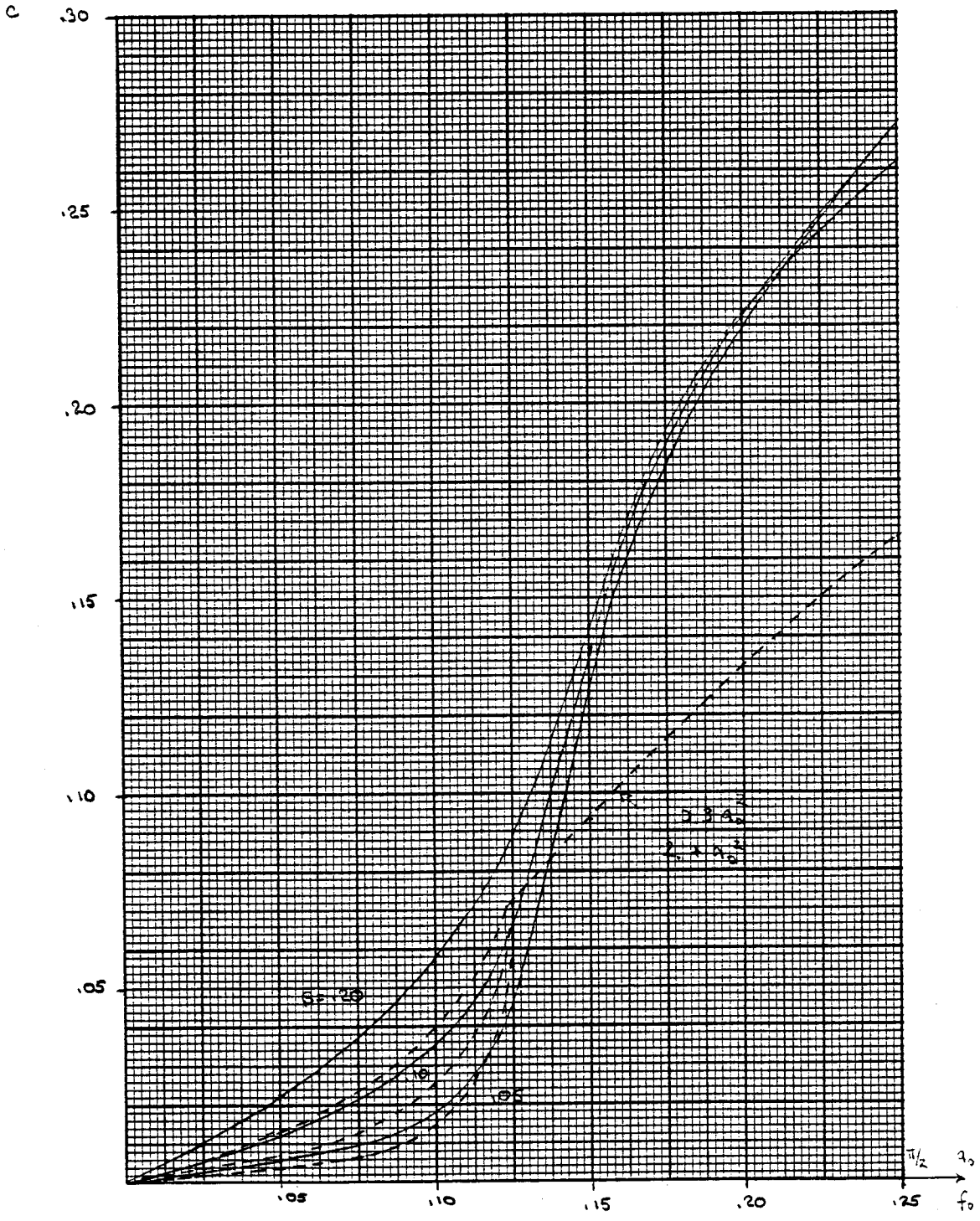

FREQUENCY (Hz)

NORMALIZED TORSIONAL STIFFNESS (IMAGINARY COMPONENT)

H/R = 2 β = .05 REGULAR MESH

FIGURE 40

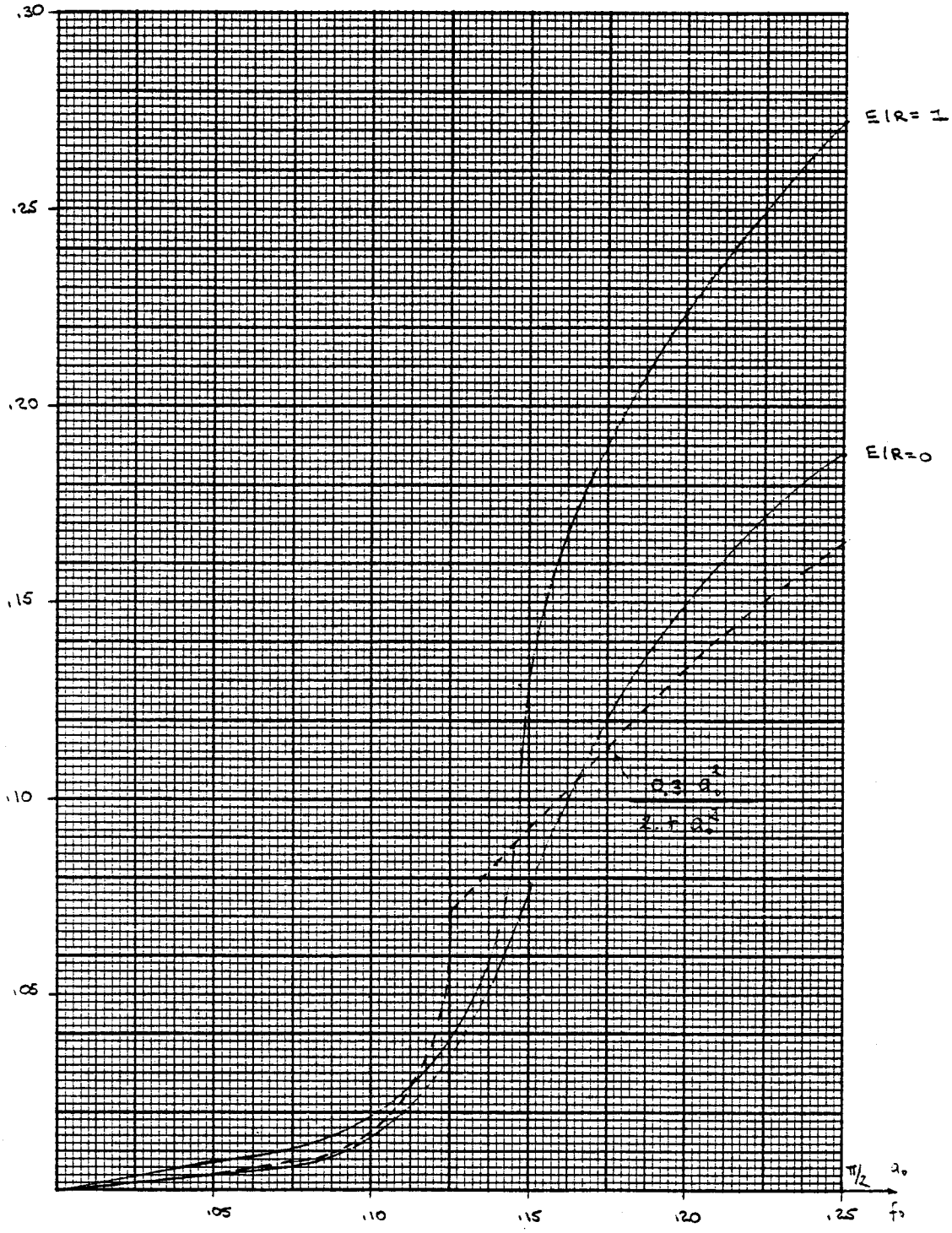

FREQUENCY (Hz)

NORMALIZED TORSIONAL STIFFNESS (IMAGINARY COMPONENT)

H/R = 3 β = .05 REGULAR MESH

FIGURE 41

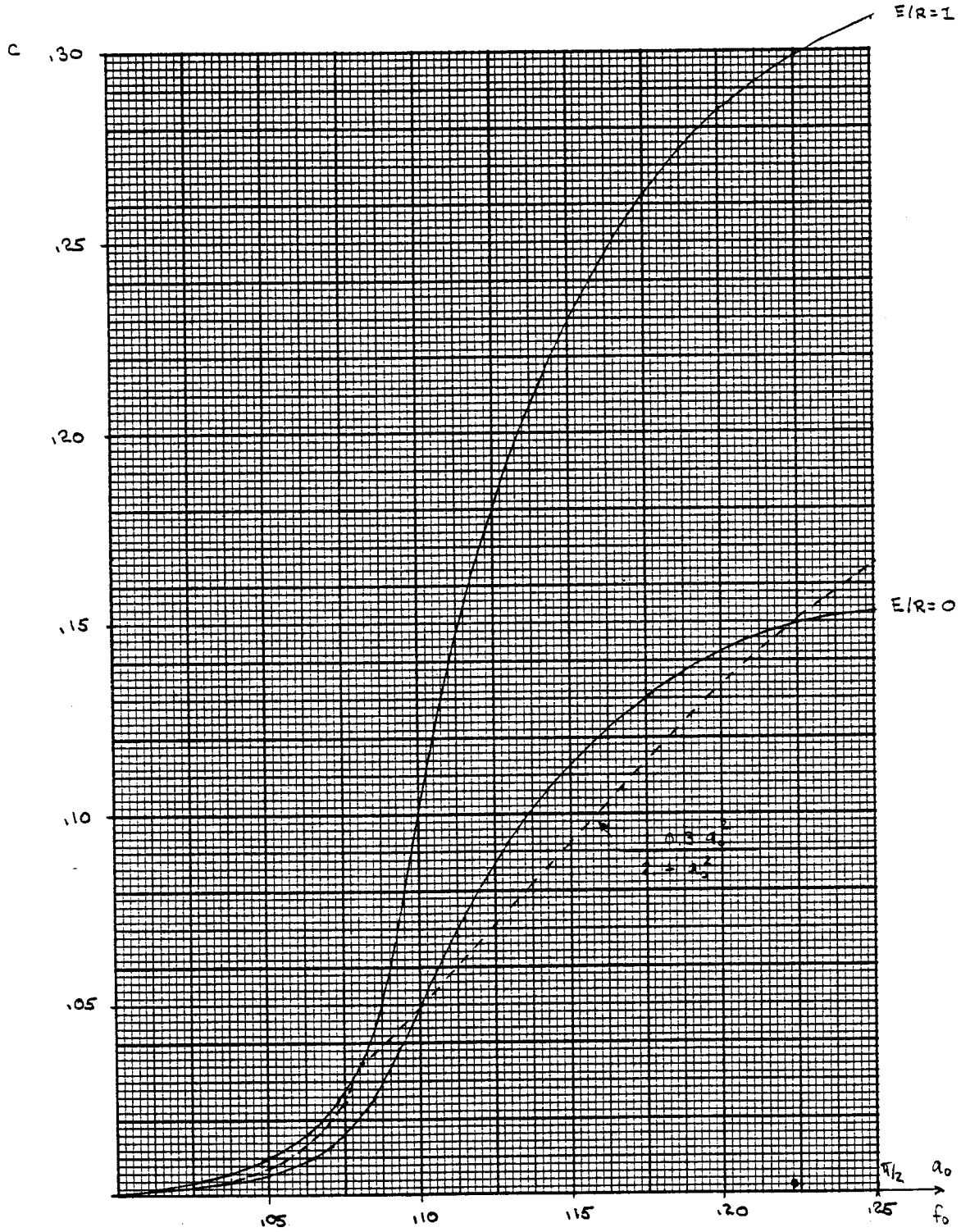

FREQUENCY (Hz)

$$c = \frac{0.67\ \beta\ \xi}{1 - (1-2\beta)\xi^2}$$

$$\xi = f/f_p < 1, \quad f_p = C_p/4H$$

Vertical Case

$$c = \frac{0.15\ \beta\ \xi}{1 - (1-2\beta)\xi^2}$$

$$\xi = f/f_s < 1, \quad f_s = C_s/rH$$

Torsional Case

These formulae are evaluated for the various cases in tables 11 and 12, and are shown as dashed lines in Figures 34 through 41. The degree of approximation is fair, considering the dependence of these components with embedment and stratum depth.

CONCLUSION

A numerical evaluation of the vertical and torsional stiffnesses of an embedded, cylindrical foundation was performed with a finite element program incorporating transmitting boundaries (12). The evaluations of the results was made in a manner similar to that employed by Elsabee (8) for the horizontal and rocking modes. The resulting empirical expressions are summarized below, including, for convenience, the results obtained by Elsabee (8).

1) Static Stiffnesses

$$K_h = \frac{8GR}{2-\nu}\left(1 + \frac{1}{2}\frac{R}{H}\right)\left(1 + \frac{2}{3}\frac{E}{R}\right)\left(1 + \frac{5}{4}\frac{E}{H}\right)$$

$$K_{h\phi} = \left(0.4\ \frac{E}{R} - 0.03\right)R\ K_h \qquad \text{(dynamic variation same as } K_h\text{)}$$

$$K_\phi = \frac{8GR^3}{3(1-\nu)}\left(1 + \frac{1}{6}\frac{R}{H}\right)\left(1 + 2\ \frac{E}{R}\right)\left(1 + 0.7\ \frac{E}{H}\right)$$

$$K_v = \frac{4GR}{1-\nu}\left(1 + 1.28\ \frac{R}{H}\right)\left(1 + 0.47\ \frac{E}{R}\right)\left(1 + \left(0.85 - 0.28\ \frac{E}{R}\right)\frac{E/H}{1-E/H}\right)$$

$$K_t = \frac{16GR^2}{3}\left(1 + 2.67\ \frac{E}{R}\right)$$

In the above formulae, $E/R \leq 1.5$, $E/H \leq 0.75$, $R/H \leq 0.5$.

2) Dynamic Stiffnesses

$$K = K^o(k + i\, a_o\, c)(1 + 2i\beta)$$

with K^o = static stiffness; k, c = stiffness functions, $a_o = \Omega R/C_s$ = dimensionless frequency ($\Omega = 2\pi f$ = circular frequency, R = radius, C_s = shear wave velocity); and β = material (hysteretic) damping of the soil.

For all modes, it is recommended to use the halfspace functions (k,c) as reported by Luco (17) or Veletsos and Wei (27), except for the function c in the low frequency range. In this range, the radiation coefficient can be estimated by

$$c = \frac{\alpha\ \beta\ \xi}{1 - (1-2\beta)\xi^2}\ ,\quad \xi \leq 1$$

with parameters α,ξ tabulated below

	α	ξ
Swaying	.65	f/f_s
Rocking	.50	f/f_p
Vertical	.67	f/f_p
Torsion	.15	f/f_s

Frequently, it is not necessary to use numerical tabulations for the halfspace curves, but it suffices to use instead the approximations (see also Fig. 40):

	k		c
Swaying	1.		0.6
Rocking	$1. - 0.2\ a_o$	$a_o < 2.5$ (*)	$0.30\ a_o^2/(1. + a_o^2)$
	0.5	$a_o \geq 2.5$	
Vertical	1.		0.85
Torsion	$1. - 0.133\ a_o$	$a_o < 3.0$	$0.30\ a_o^2/(2. + a_o^2)$
	0.6	$a_o \geq 3.0$	

(*) For $\nu \geq 0.45$, use first expression for every a_o

These approximations are particularly useful in quick estimates of soil-structure interaction effects.

STIFFNESS COEFFICIENTS FOR A SURFACE FOOTING OVER AN ELASTIC HALF SPACE $\nu = 1/3$

FIGURE 40

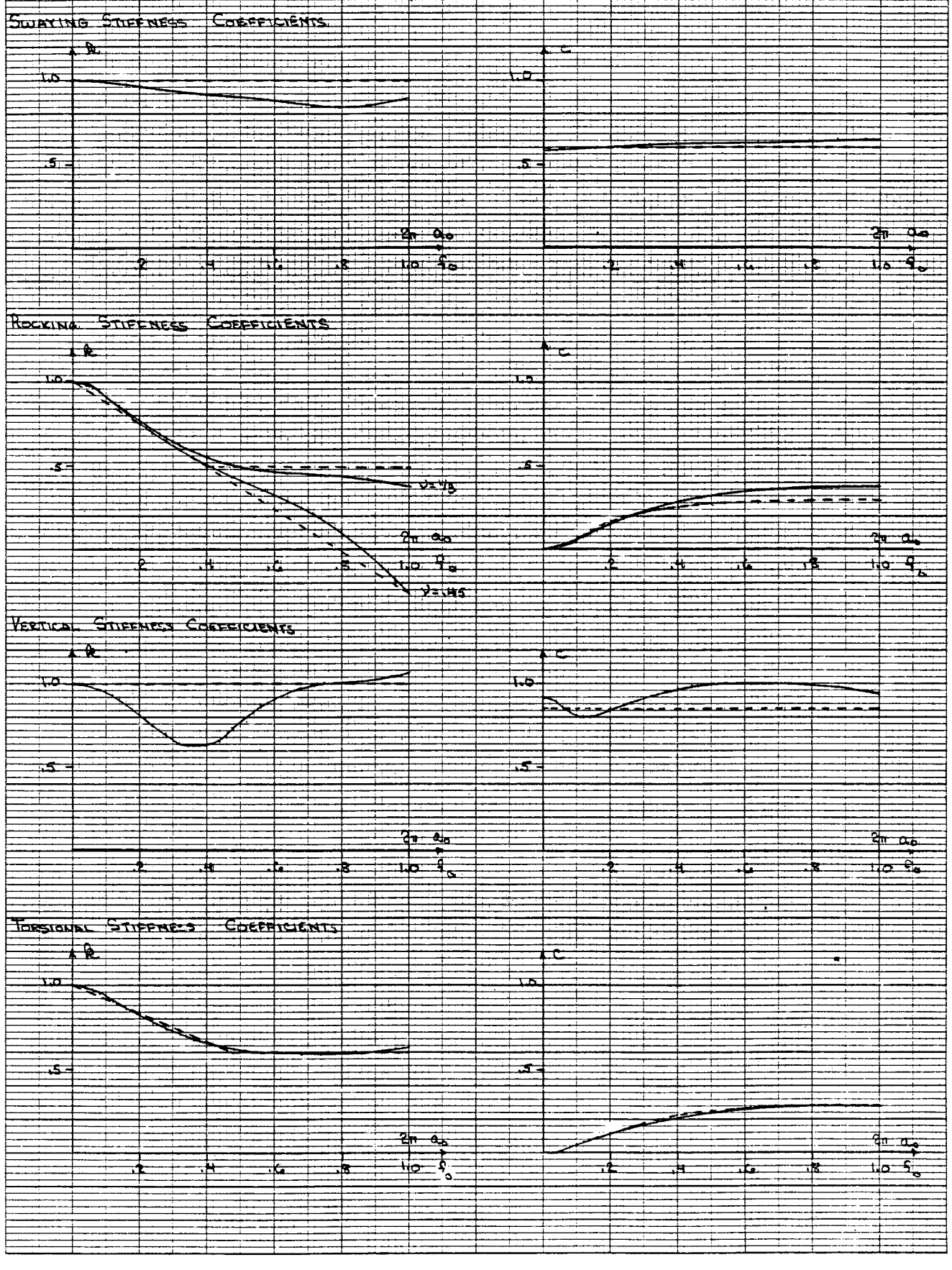

REFERENCES

1. Anandakrishnan, M., and Krishnaswamy, N.R.: "Response of embedded footings to vertical vibrations," Jour. of Soil Mech. Found. Div., ASCE, Vol 99, No. SM10, Oct. 1973, pp. 863-883.

2. Apsel, R.J., Luco, J.E., "Torsional Response of Rigid Embedded Foundations," Journal of the Engineering Mechanics Division, ASCE, December 1976, p. 957-970.

3. Baranov, V.A., "On the calculation of excited vibrations of an embedded foundation," (in Russian), Voprosy Dynamiki: Prochnocti, No. 14, Polytechnical Institute of Riga, 1967, pp. 195-209.

4. Beredugo, Y.O., "Vibrations of embedded symmetric footings," Ph.D. Dissertation, Univ. of Western Ontario, Canada, 1971, 247 pp.

5. Bielak, J., "Dynamic Behavior of Structures with Embedded Foundations," Earthquake Engineering and Structural Dynamics, Vol. 3, No. 3, Jan.-March, 1975.

6. Bycroft, G.N., "Forced vibrations of a rigid circular plate on a semi-infinite elastic space and on an elastic stratum," Philos. Trans., Roy. Soc. London, Series A, No. 948, Vol 248, Jan. 1956, pp. 327-368.

7. Chang Liang, V., "Dynamic Response of Structures in Layered Soils," Research Report R74-10, Civil Engineering Department, M.I.T., Jan. 1974.

8. Elsabee, F., "Static Stiffness Coefficients for Circular Foundations Embedded in an Elastic Medium," Thesis presented to the Civil Engineering Department of M.I.T. in partial fulfillment of the requirements for the M.S. degree, 1975.

9. Erden, S.M., "Influence of shape and embedment on dynamic foundation response," Ph.D. Dissertation, Univ. of Massachusetts, March 1974, 437 pp.

10. Johnson, G.R., Christiano, P., and Epstein, H.I., "Stiffness coefficients for embedded footings," Proc., ASCE Power Div. Specialty Conf., Denver, Col., Aug. 1974, pp. 499-523.

11. Kaldjian, J.M., "Torsional stiffness of embedded footings," Jour. Soil Mech. Found. Div., ASCE, Vol 97, No. SM7, July 1971, pp 969-980.

12. Kausel, E., "Forced vibrations of circular foundations on layered media," Ph.D. Dissertation, Massachusetts Institute of Technology, Jan. 1974, 240 pp.

13. Kausel, E., Whitman, R.V., Morray, J.P., and Elsabee, F., "The Spring Method for Embedded Foundations," Nuclear Engineering and Design, 48 (1978), pp 377-392.

14. Krizek, R.J., Gupta, D.C. and Parmelee, R.A., "Coupled sliding and rocking of embedded foundations," Jour. Soil Mech. Found. Div., ASCE, Vol 98, No. SM12, Dec. 1971, pp 1347-1358.

15. Luco, J.E., "Impedance Functions for a Rigid Foundation on a Layered Medium," Nuclear Engineering and Design, 31 (1974) pp 204-217.

16. Luco, J.E., "Torsion of a Rigid Cylinder Embedded in an Elastic Half-Space," Journal of Applied Mechanics, Vol 43, Series E, No. 3, Sept. 1976, pp 419-423,

17. Luco, J.E. and Westmann,R.A., "Dynamic response of circular footings," Jour. Engrg. Mech. Div., ASCE, Vol 97, No EM5, Oct. 1971, pp 1381-1395.

18. Lysmer, T., and Waas, G., "Shear waves in plane infinite structures," Jour. Engrg. Mech. Div., ASCE, Vol 98, Feb. 1972, pp 85-105.

19. Novak, M., "Vibrations of embedded footings and structures," Preprint 2029, ASCE, National Struct. Eng. Meeting, San Francisco, Calif., April 1973, 25 pp.

20. Novak, M. and Beredugo, Y.O., "The effect of embedment on footing vibrations," Proc. First Canadian Conf. Earthq. Engrg. Research, Vancouver, B.C., May 1971, pp 1-14.

21. Novak, M. and Sachs, K., "Torsional and coupled vibrations of embedded footings," Int. Jour. Earthq. Engrg. Struct. Dyn.,Vol 2, No. 1, July-Sept., 1973, pp 11-33.

22. Reissner, E., "Stationare, axialsymmetrische durch eine schuttelude masse erregte schwingungen eines homogenen elastischen halbraumes," Ingenieur - Archiv, Vol 7, Part 6, Dec. 1936, pp 381-396.

23. Reissner, E. and Sagoci, H.F., "Forced Torsional Oscillations of an Elastic Halfspace," Jour. App. Phys., Vol 15, No. 9, pp. 652-662.

24. Stokoe, K.H. II, "Dynamic response of embedded foundations", Ph.D. Dissertation, Univ. of Michigan, Jan. 1972, 251 pp.

25. Tajimi, H., "Dynamic analysis of a structure embedded in an elastic stratum," Proc. 4th World Conf. Earthq. Engrg., Santiago, 1969, pp 53-69.

26. Urlich, C.M. and Kuhlemeyer, R.L., "Coupled rocking and lateral vibrations of embedded footings," Can. Geotech. Jour., Vol 10, No. 2, May 1973, pp 145-160.

27. Veletsos, A.S. and Wei, Y.T., "Lateral and rocking vibration of footings," Jour. Soil Mech. Found. Div., ASCE, Vol. 97, No. SM9, Sept. 1971, pp 1227-1248.

28. Waas, G., "Linear two-dimensional analysis of soil dynamics problems in semi-infinite layer media," Ph.D. Dissertation, Univ. of California, Berkeley, 1972.